Accepted Manuscript

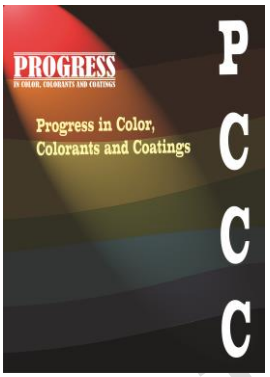

Title: Harnessing Herbaceous Plants as an Eco-Friendly Source of Carbon-Based Adsorbents for Water Remediation: A Review

Authors: Noor Albayati, Hind Ahmed, Muhsin J. Jweeg, Mohammed Kadhom, Ghassan Abdullah, Suhaib Salih

Manuscript number**: PCCC-2409-1309**

To appear in: Progresss in Color, Colorants and Coatings

Received: 14 July 2024

Final Revised: 24 Sep 2024

Accepted: 30 Sep 2024

Please cite this article as:

N. Albayati, H. Ahmed, M.J. Jweeg, M. Kadhom, G. Abdullah, S. Salih, Harnessing Herbaceous Plants as an Eco-Friendly Source of Carbon-Based Adsorbents for Water Remediation: A Review, Prog. Color, Colorants, Coat., 18 (2025) XX-XXX.

Harnessing Herbaceous Plants as an Eco-Friendly Source of Carbon-Based Adsorbents for Water Remediation: A Review

Noor Albayati[1], Hind Ahmed[2], Muhsin J. Jweeg[3], Mohammed Kadhom[2,*], Ghassan Abdullah[4], Suhaib Salih[4]

[1] Department of Chemical Engineering, College of Engineering, University of Baghdad, P.O. Box: 10071, Baghdad, Iraq.

[2] Department of Environmental Science, College of Energy and Environmental Science, Alkarkh University of Science, P.O. Box: 10081, Baghdad, Iraq.

[3] College of Technical Engineering, Al-Farahidi University, P.O. Box: 10070, Baghdad, Iraq.

[4] Department of Chemical Engineering, College of Engineering, Tikrit University, P.O. Box: 34001, Saladin, Iraq.

* Corresponding Author Email: kadhom@kus.edu.iq, mohammedkadhom@gmail.com

Abstract

The water deficit by 2050 is anticipated to increase from 85 km³ to 283 km³ annually, which puts the world in a real threat if no practical solutions are introduced. This research explores the diverse adsorption potential of herbaceous plants, particularly Rosaceae, Paeoniaceae, Malvaceae, and Asteraceae, to improve eco-friendly and efficient water remediation technologies. The study catalogs 22 herbaceous plants using Scopus data and focuses on pollutant adsorption. Rose waste (especially ultimate rose pulp) and rose flower biomass may remove wastewater pollutants. Novel biomass treatments like coating, pyrolyzing, soaking in activating solutions, and synergizing with additives

increase pollutant water adsorption. Spent Alchemilla vulgaris leaves absorb methylene blue dye well. Paeoniaceae, represented by Paeonia ostii seed coats, showed novel heavy metal adsorbents with excellent capacities and reusability. Hibiscus species of Malvaceae show phytoremediation potential, removing dyes and adsorbing Safranin dye with activated carbon from Hibiscus cannabinus. In the Asteraceae family, sunflower-based adsorbents for water treatment were studied for various pollutants using biochar modification, chemical treatment, and nanoparticle incorporation. The exceptional adsorption properties of biochar, the cost-effective production of activated carbon, the versatility of sunflower straw-activated carbon, and the use of nanoparticles-coated sunflower husk were found for simultaneous antibiotics adsorption and dye removal. Marigold and Chamomile, Asteraceae plants, are versatile environmental adsorbents. This comprehensive research uses herbal-based adsorbents due to their efficacy, economic viability, and environmental sustainability.

Keywords: herbaceous plants; adsorption; Rosaceae; Paeoniaceae; Malvaceae; Asteraceae

1- Introduction

Humans cannot survive without water; freshwater shortages and excessive water resource usage are major global issues that are getting worse [1]. Around the world, an estimated 2.2 billion people lack access to pure water supplies, while approximately 800 million people lack even fundamental access to drinking water. Due to the effects of climate change, Southeast Asia is especially vulnerable to experiencing water scarcity and rising water demand [2].

The projected water resource availability in the Middle East and North Africa (MENA) region is subject to fluctuations caused by multiple causes, such as climate change, population expansion, economic progress, and environmental concerns. To examine the impact of these changes, Droogers et al. employed a two-stage modeling approach. They found that by 2050, the total water need in the region will rise to 393 km^3 yr^{-1}, while the overall water lack will increase to 199 km^3 yr^{-1} under the average climate change projection. This represents a substantial rise of 157 km^3 yr^{-1} in water shortage, resulting from a 50% surge in water demand combined with a 12% reduction in water supply. Uncertainty, based on the output of nine applied General Circulation Models (GCMs), it was suggested that the projected water shortage for 2050 may increase by 333%. According to the study, changing socioeconomic conditions account for 78% of water scarcity, while climate change accounts for 22% [3].

Multiple techniques are utilized to cleanse water contaminated with dyes, such as filtering, chemical coagulation and precipitation, ultrasonic and biological breakdown, chemical oxidation, electrochemical removal and electrocoagulation, photocatalysis, and adsorption [4, 5]. Among these methods, adsorption is presented as the most advantageous because of its straightforward operation, high efficiency, ease of implementation, and limited undesired byproducts [6]. Adsorption refers to the binding of specific substances or ions (adsorbates) onto both the internal and external surfaces of a solid material known as an adsorbent. Over time, various materials were utilized as adsorbents to capture different compounds [7]. In addition to the mentioned advantages, this technology aims to use affordable and renewable adsorbents [8]. One significant advantage of adsorption over other purifying processes is its lower cost. Unlike other

technologies, which can cost anywhere from \$10 to \$450/m^3, adsorption can treat water volumes ranging from \$5 to \$200/m^3 [9]. When comparing the advantages and disadvantages of each approach, adsorption emerges as the most favorable choice, where it was investigated by research teams [10].

Natural water can be unfitting for human consumption because of the presence of various contaminants. Mainly, the harmful effects of heavy metals (HMs) and dyes prompted much research. Incorrect chemical disposal, agricultural runoff, and industrial effluent are potential entry points for these contaminants into water sources. Figure 1 (a) shows a diagram of the common kinds of contaminations present in water. The presence of heavy metals such as chromium (Cr), selenium (Se), iron (Fe), mercury (Hg), copper (Cu), vanadium (V), cadmium (Cd), zinc (Zn), nickel (Ni), cobalt (Co), lead (Pb), and arsenic (As) poses significant threatening to human health and other living organisms because of their toxicity. Removing these HMs from wastewater serves a dual purpose: it eliminates their harmful effects and allows for the recovery of valuable materials [11].

While the industrial revolution has brought advancements in human life and healthcare, it has also resulted in environmental deterioration, posing significant challenges for the planet [12]. The textile industry is a major global industry that contributes to this issue by releasing substantial amounts of dyes, chemicals, and hazardous metals/elements into wastewater. However, due to the absence of an accurate database, it is difficult to calculate the total quantity of discharged dyes. But, it is known they are vast numbers as many countries heavily rely on the fabric and textile industries for their economies [13]. Reports suggest that there are over 100,000 types of dyes available, primarily used in the clothing industry [14]. Consequently, it is anticipated that

more than 300,000 tons/ year of dyes are released into streams from the textile industry alone, in addition to other industries [15]. These pollutants have been identified as toxic, carcinogenic, and harmful, resulting in various health issues such as allergies, skin irritation, breathing difficulties, sweating, confusion, vomiting, nausea, mutations, headaches, and high blood pressure [16]. Dyes can be categorized into three groups: cationic, anionic, and nonionic, each containing multiple types of dyes. Anionic dyes include reactive, acid dyes, and direct, while cationic and nonionic dyes are represented by basic and dispersed dyes, respectively [17].

Many groups, including ours, have employed different materials as adsorbents, involving new class materials such as covalent organic frameworks (COFs), metal organic frameworks (MOFs), carbon-derived materials, and MXenes [18]. Yet, biomass-based materials still have many merits that other materials cannot beat, mainly their low cost, eco-friendship, abundance, simple modification, and easy handling and processing [19]. The cost of utilizing biowaste as a removal material is significantly low compared to other options. For example, black liquor waste is priced at $1 per 1,000 kg, while lignin and activated carbon are priced at $60 and $100 per 1,000 kg, respectively. Moreover, rice husk, which is available in massive quantities (over 100 million tons per year), has the highest cost lower than $0.025 per kg. It is worth noting that clay is another cost-effective option, with prices ranging from $0.04 to $0.12 per kg [20].

Herbaceous plants encompass a wide array of flowering plants that lack persistent woody stems. They exhibit immense ecological importance in terrestrial and aquatic ecosystems worldwide. These plants serve as primary producers, contributing significantly to carbon fixation and the provision of habitat and food sources for

numerous organisms [21]. Furthermore, herbaceous plants play vital roles in nutrient cycling, soil stabilization, erosion control, and water filtration, enhancing overall ecosystem functioning. Herbaceous plants form the foundation of many ecosystems, providing essential ecosystem services. They contribute to pollination dynamics and foster biodiversity by providing critical habitats for various animal species, including insects, birds, and mammals [22]. The diversity of herbaceous plants also supports genetic diversity, promoting resilience against environmental disturbances. Additionally, many herbaceous species exhibit specialized adaptations, such as drought tolerance or shade tolerance, which further contribute to ecosystem resilience. However, many of them are seasonal, and their parts dry and go back to the environment [23].

This review examines 22 herbaceous plants and categorizes them based on their families. Among these plants, some have already been employed in adsorption studies, while others have not. For those utilized, we present various studies that explore their efficacy in removing different types of pollutants. Given the abundance of these plants across the planet, irrespective of their geographical distribution, utilizing the residual parts of these plants after the flowering season could serve as a cost-effective source of adsorbents. Figure 1 (b) shows a diagram on the commonly used herbaceous plants in adsorption in the last 5 years. Hence, we strongly encourage researchers and scientists to investigate the potential of these plants' waste for direct use as adsorbents, as well as their indirect use by preparing adsorbents.

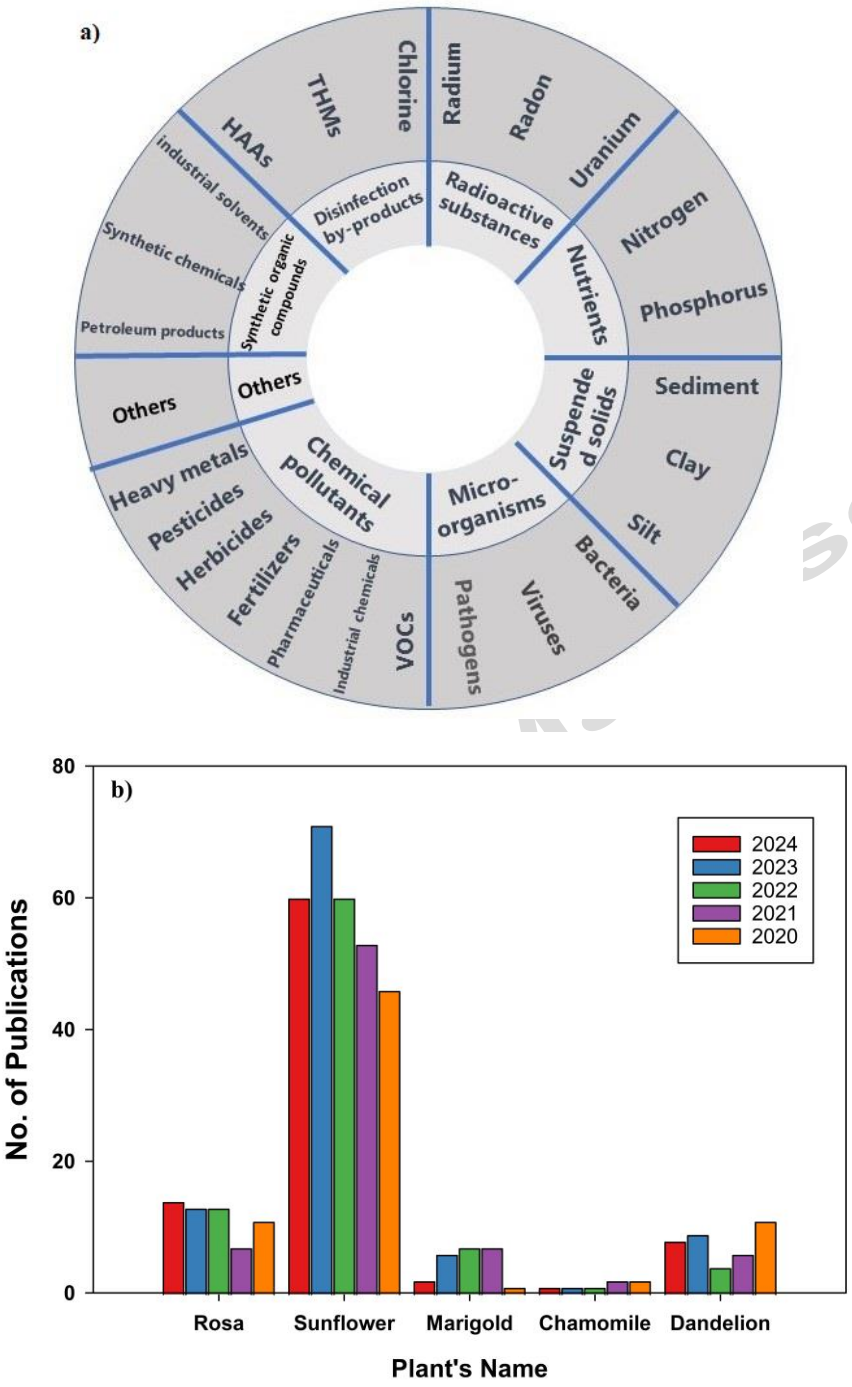

Figure 1. (a) A diagram for the possible types of contaminations in water, where VOCs: volatile organic compounds, THMs: trihalomethanes, and HAAs: haloacetic acids, (b) A diagram on number of publications for selected 5 plants in the last 5 year, data were collected on Aug 15th, 2024 based on Scopus database searching in the article title, abstract, and keywords field for the plant name and "adsorption". [The figure was prepared by the authors].

2- Studied Herbaceous Plants and Targeted Pollutants

2-1 Classification of Herbaceous Plant Species

The names of plants and their classification families were listed in Table S-1, where they were explored using the Scopus database. The table contained 22 herbs that were classified into 4 families based on their natural classification; the included families are Rosaceae, Paeoniaceae, Malvaceae, and Asteraceae. The search included the use of the plants' common and scientific names in different search fields. It is worth noting that not all research papers were reported in the case of multiple published works dealing with the same pollutant.

2-2 Target Pollutants

This review paper classified the targeted pollutants into three primary categories: heavy metals, dyes, and organic compounds, including antibiotics, catechol, and resorcinol. The heavy metals considered in this study include lead (Pb), americium (Am), strontium (Sr), arsenic (As), copper (Cu), iron (Fe), chromium (Cr), cadmium (Cd), nickel (Ni), mercury (Hg), and zinc (Zn). These metals are known for their environmental persistence and potential for bioaccumulation, as illustrated in our previous study [20]. These metals can be highly toxic even at low concentrations, affecting various biological systems and posing significant risks to both ecosystems and human health. They are commonly found in industrial discharges, mining operations, and agricultural runoff, making them critical targets for remediation efforts [11].

The dyes included in the analysis contains methylene blue (MB), congo red (CR), methyl red (MR), malachite green (MG), crystal violet (CV), Reactive Blue 221

(RB221), Red X-5GN (RB14), acid fuchsin, and safranin. These dyes are extensively used in textiles, paper, and printing industries. Similar to heavy metals, dyes are often resistant to biodegradation and can persist in water bodies, which lead to severe environmental issues, including aquatic toxicity, inhibition of photosynthesis in aquatic plants, and potential carcinogenic effects on humans [15]. Antibiotics like levofloxacin (LEV), meropenem (MER), and tetracycline (TC) are classified as emerging contaminants due to their increasing presence in water bodies, often as a result of improper disposal and agricultural runoff. These compounds contribute to the development of antibiotic-resistant bacteria, posing a significant threat to public health and environmental safety [24]. Finally, Catechol and resorcinol, classified as organic compounds, are widely used in industrial applications, including the production of dyes, resins, and pharmaceuticals. They are known for their toxicity and potential to cause environmental harm, particularly through water contamination. Their presence in industrial effluents necessitates effective treatment strategies to mitigate their impact on both human health and the environment [25].

3- Adsorption via Herbaceous Plants

In this section, we will expound upon the utilization of herbaceous vegetation as adsorbents for various categories of pollutants, as delineated in Table S1, which provides a classification of these herbs based on their respective plant families. It is imperative to note that a subset of the listed plants were not subjected to prior investigations and remained untapped for adsorption applications. In contrast, certain plants have garnered extensive attention and deployment in this regard. Consequently, we present studies that

have harnessed these plant varieties to eliminate dyes, heavy metals, pharmaceutical agents, and other environmental contaminants, organized according to their corresponding botanical families.

3.1. Rosaceae

3.1.1. Rose

Rose could be the most famous plant of its family. However, rose concrete, a viscous substance composed of hexane and essential oils extracted from rose petals, serves as a valuable ingredient in various applications. The production of rose concrete requires a substantial quantity of rose flowers, approximately 350 kg per 1 kg of the final product. Through the process of hexane extraction, the flowers yield rose concrete while retaining insoluble pigments. Notably, there is an excess of more than 2275 tons of non-polar solvent-extracted flowers remaining after the extraction procedure, which makes the leftover residue unusable and classified as garbage.

However, this rose waste was applied as a natural source to treat polluted water; here, Karaboyaci used rose waste to adsorb lead (Pb^{2+}) from wastewater. Experimental investigations demonstrate the efficacy of evaluating the final residue obtained from rose processing as a potential adsorbent, known as ultimate rose pulp. This is particularly valuable as the ultimate rose pulp exhibits the ability to adsorb 70 parts per million (ppm) of Pb^{2+} ions from an aqueous solution containing 100 ppm of Pb^{2+} when the pH is maintained above 5.5 [26]. In another study, Aman et al. studied the potential of rose flower biomass as a biosorbent for the removal of Hg(II), Cr(III), and Zn(II) metals from industrial wastewater. Several variables were examined, including untreated biomass, biomass treated with acid or base, metal ion concentration, pH, contact time, and biomass

dosage. The results indicated that maximizing the biomass dosage and metal ion concentration enhanced the biosorption process. The pH of the solution had a crucial role, with all metals exhibiting high adsorption capacities at moderate acidic to moderate basic pH levels of 6 to 10. Conversely, the uptake of metals was significantly reduced at low pH values. The contact time had a minor impact on zinc adsorption, but it was crucial for mercury removal. Base treatment of the biomass proved beneficial for the adsorption of zinc and mercury. The adsorption of three HMs on rose biomass followed both the Langmuir and Freundlich isotherms, suggesting multiple mechanisms at operation. Furthermore, the adsorption process was best described by pseudo-second-order kinetics, indicating a rate-limiting step. In this study, at a metal ion concentration of 100 ppm, the adsorption capacities of chromium, mercury, and zinc were 5.26, 7.62, and 4.07 mg/g, respectively. When the HMs' concentration was reduced to 50 ppm, the adsorption capacity was reduced to 4.07 mg/g for chromium, 6.76 mg/g for mercury, and 3.33 mg/g for zinc. Furthermore, at a lower metal ion concentration, the adsorption capacity further decreased. However, experimental results revealed that the highest adsorption capacity of chromium was achieved at 6.01 mg/g after 120 min of contact. While for mercury and zinc, it was observed after 150 min with values of 2.66 mg/g and 0.34 mg/g, respectively [27].

The final example of using rose waste is the employment of its leaves with polypyrrole (PPy) to remove Pb (II) and Cd (II) from polluted water [28]. Through a chemical oxidative route, the rose leaf was effectively upgraded by coating it with PPy. Extensive characterization of the resulting rose leaf/polypyrrole (RL/PPy) composites was conducted, focusing on conductivity, morphology, and chemical structure properties.

The FTIR results provided spectra that supported the generation of RL/PPy composites, while both FTIR and SEM analyses demonstrated the complete coverage of the rose leaf surface by PPy. Compared to pure polypyrrole, the composite showed a greater conductivity (1.8215 S/cm). The primary mechanism responsible for the conductivity of PPy is a p-type (bipolaron) process. Because the PPy structure has an electron pair on nitrogen atoms, this process allows electrons to hop across polymer chains. The flow of anions and cations into and out of the polymer structure also affects the conductivity due to the intricate processes that comprise the movement of ions and electrons inside the polymer network [29]. An electron pair from the nitrogen (N) atom of the conducting polymer interacts with the Pb(II) ions to produce the adsorption of metal cations on the produced composite. This interaction shows how the composite material may efficiently collect and immobilize Pb(II) ions by employing an electron-sharing mechanism [30]. Varying the adsorbent dose, stirring speed, contact length, pH, and metal solution concentration led to identifying the best conditions for adsorption were found. The RL/PPy composite's ability to terminate Pb(II) and Cd(II) from wastewater was subsequently tested using ICP-OES. To analyze the adsorption data, both the Langmuir and Freundlich models were utilized. Because the Freundlich model was better in agreement with the practical findings, it follows that there ought to be several adsorption sites that possess acceptable adsorption properties. For the optimal Pb(II) removal, pH of 8.0, 0.2 g/50 mL of adsorbent, an initial concentration of 1.5 mg/L, a stirring speed of 300 rpm, and a time of 15 min were required. Under these conditions, the maximum adsorption percentage (Ads%) with only RL was 56%, while with RL/PPy it was 81%. Similarly, for Cd(II) removal, the optimal conditions included a pH of 5.0, a dosage of

0.2 g/50 mL, a stirring speed of 300 rpm, an initial concentration of 75 mg/L, and a time of 45 min. The Ads% achieved with RL was 85%, while it reached to 92% with RL/PPy.

3.1.2. Alchemilla

Alchemilla is another plant of the Rosaceae family that was utilized for adsorption, where spent alchemilla vulgaris leaves were utilized to adsorb methylene blue (MB) from an aqueous solution [31]. The factors that influenced the adsorption efficiency included initial pH, adsorbent mass, initial dye concentration, temperature, and particle size. The Freundlich, Temkin, BET, and Langmuir models were compatible with the adsorption data. The maximum removal efficiency obtained was 87.85% when the adsorbent concentration was 0.5 g/L and the dye concentration was 10 mg/L. The experimental results were in excellent agreement with the Freundlich isotherm model. Methylene blue adsorption followed a pseudo-second-order kinetic rate expression, according to the kinetic analysis. Furthermore, the reaction entropy (ΔS^o) was -12.283 J/mol and the reaction enthalpy (ΔH^o) was 8.54 kJ/mol. With an E_a of 25.535 kJ/mol, it is concluded that physical interactions are the main drivers of the exothermic adsorption process.

Findings indicated that reducing the particle size of the adsorbent led to an improvement in the removal efficiency, although the differences between the studied particle sizes were not significant. Enhancing the adsorbent dosage and decreasing the dye concentration were found to enhance the dye removal efficiency. Moreover, as the temperature rose, the adsorption efficiency decreased while the adsorption rate enhanced; however, the thermodynamic analyses revealed that the adsorption process was spontaneous and exothermic.

3.2. Paeoniaceae

Perennial plants, encompassing a variety of forms such as herbs, half-shrubs, and shrubs, exhibit stems that are either herbaceous or woody, typically branching from cataphylls. These plants feature thickened rhizomes and roots that can take on a napiform or bulbous morphology. Their leaves are notably large and deciduous, arranged alternately, and may be ternately, dissected, or pinnately compound. The flowers of these plants are quite sizable, typically solitary, and emerge at the terminals of the main axis or branches. Their flowering occurs in the spring to early summer, and they bear fruit in the summer to fall. This botanical description pertains to a singular genus consisting of approximately 40 species, with the majority of them being located in warm-temperate Eurasia, and two species are found in western North America [32].

In research from Ren's group, a new adsorbent, phosphoric acid-modified Paeonia ostii seed coats (PA-PSC), was synthesized through low-temperature pyrolysis, demonstrating remarkable efficiency in the removal of Cu(II) from the solutions. The equilibrium adsorption capacity (q_e) of PA-PSC exhibited a substantial four-fold increase when compared to raw PSC, highlighting its effectiveness as an adsorbent. Analysis utilizing XPS and FTIR techniques assumed that the adsorption of Cu(II) onto PA-PSC mainly occurred through electrostatic forces and complexation mechanisms. The equilibrium data and adsorption kinetics were well-fitted with Freundlich and pseudo-second-order models, respectively. Thermodynamic analysis indicated that the process was endothermic, spontaneous, and chemical in nature. Additionally, the reusability test further confirmed the practical utilization of PA-PSC as a notable adsorbent for the effective termination of Cu(II) from wastewater [33]. In a separate study, the same

researchers discovered that IDA-PSC, which stands for iminodiacetic acid-functionalized Paeonia ostii seed coats, was able to purify water from copper ions. Extensive characterization of IDA-PSC using FTIR, BET, XPS, and SEM investigations revealed its structural and morphological characteristics. Adsorption was robust in the presence of low pH values and competing ions such as Na^+ and Ca^+. The Pseudo-second-order model adequately described the adsorption kinetics at 25°C, whereas the Langmuir model accurately depicted the isotherms. The maximum monolayer adsorption capacity was 36.6 mg g^{-1}. Based on thermodynamic study, the adsorption is endothermic and occurs spontaneously. The adsorption mechanism relied heavily on surface functional groups containing nitrogen and oxygen. ion exchange, electrostatic attraction, intraparticle diffusion, and surface complexation were the processes that contributed to Cu(II) adsorption. Additionally, the IDA-PSC demonstrated remarkable reusability for six consecutive cycles, highlighting its promising capabilities for HMs removal from water-based solutions [34].

The potential of alkali-pretreated Paeonia ostii seed coats (AP-PSC) as a highly efficient adsorbent for the removal of MB dye from wastewater was investigated. Important process parameters, such as alkali concentration, liquid-solid ratio (LSR), and pretreatment duration, were adjusted by the researchers using an orthogonal array design. The results showed that the best pretreatment conditions were 0.8% (w/w) of NaOH, 0.35 L g^{-1} of LSR, and 50 min of treatment time. With the highest adsorption capacity of 368.2 mg g^{-1} for MB at 25°C, equilibrium and kinetic tests proved that the experimental results were well characterized by the Langmuir isotherm and Pseudo-second-order models. Thermodynamic analysis revealed that the adsorption process was endothermic,

physical, and spontaneous. Importantly, the adsorption process was affected by multiple interactive mechanisms, including hydrogen bonds, Van der Waals forces, and ion exchange [35].

3.3. Malvaceae

Medicinal plants, also referred to as medicinal herbs, have played a significant role in traditional healing practices since ancient civilizations. These plants produce a wide spectrum of chemical compounds that serve diverse purposes, such as defense against fungi, insects, diseases, and herbivores. Many of these plants contain phytochemicals with ability or established biological activities [36]. However, owing to the multitude of phytochemicals present in a single plant, the efficacy of using the entire plant remains uncertain [37]. Hibiscus sabdariffa L., frequently known as roselle and a member of the Malvaceae family, is extensively cultivated in numerous countries, especially in developing regions. This plant species, distinguished by its visually appealing flower, is just one of 300+ recognized species found in subtropical and tropical areas across the earth. Originally indigenous to areas spanning from India to Malaysia, it boasts a rich history of cultivation and early spread to Africa. Presently, it is grown in a variety of countries including Nigeria, Sudan, Mexico, Egypt, Saudi Arabia, the West Indies, Taiwan, and Central America [38] [39].

The investigation into the phytoremediation potential of the terrestrial plant Hibiscus rosa-sinesis for the removal of MB dye from aquatic systems has yielded promising results. Through systematic studies, various crucial parameters such as initial dye concentration, interaction time, and pH were optimized to unlock the full remediation

potential of H. rosa-sinesis in treating MB-contaminated wastewater. The highest decolorization efficiency, reaching an impressive 86% for a 10 mg L^{-1} dye concentration, was achieved at a slightly acidic pH of 6. The kinetics of the adsorption process were well-described by the pseudo-first-order model, with a correlation coefficient (R^2) of ≥ 0.96, while the Langmuir adsorption isotherm model exhibited an excellent fit with R^2 ≥ 0.99. The FTIR analysis provided valuable insights, confirming the electrostatic interaction between functional groups such as O–H, C–O, and C–H in H. rosa-sinesis and N^+ present in MB during adsorption [40].

In another study, the development of a low-cost and environmentally friendly bio-based activated carbon (AC) derived from Kenaf (Hibiscus cannabinus) was achieved [41]. Through a series of activation processes involving KOH treatment and carbonization, the SEM photos demonstrated a notable increase in surface porosity, which is crucial for enhancing the adsorption capabilities of the material. The optimization of multiple parameters, like pH, initial dye concentration, adsorbent dosage, and temperature revealed that a complete removal of MB was obtained at pH 11.0, an adsorbent dosage of 0.2 g/L, an initial dye concentration of 50 mg/L, and a temperature of 30 °C. Furthermore, the kinetic and isotherm studies supported the effectiveness of Kenaf-based activated carbon, showing that the adsorption process followed the pseudo-second-order model and Langmuir isotherm, respectively.

Another study presented the potential of Acid Activated Hibiscus Sabdariffa Nano Carbon (AHSNC) as an efficient adsorbent to clean aqueous solutions from Safranin dye. The target pollutant was safranin dye, which is widely utilized in many different sectors. The study examined many important factors and found that the optimal adsorbent dosage

and contact time gave AHSNC excellent adsorption. Adsorption followed the pseudo-second-order kinetic model, and the Freundlich isotherm and Langmuir models explained the equilibrium. The study also showed how pH and solution temperature affect dye removal by analyzing their effects on adsorption [42].

A related investigation showed an encouraging dye effluent treatment method for Congo red dye. A hybrid approach using AC as an adsorbent and natural coagulant from Hibiscus sabdariffa seeds was utilized to remove color efficiently. The study examined the beginning dye concentration and pH. Based on the Response Surface Methodology (RSM) analysis and optimization, the research achieved 96.67% efficiency. This revealed the optimal dye removal conditions [43].

An example of HM removal was applying Hibiscus mutabilis leaf powder as an alternative adsorbent for chromium removal from electroplating industrial effluent. There were high concentrations of chromium, total solids, suspended solids, and acidity in the collected trash from the electroplating industry. To evaluate the efficacy of chromium removal, batch studies were performed using several doses of dried and powdered Hibiscus mutabilis leaves and different contact durations. The findings also showed that greater doses of leaf powder and longer contact durations improved chromium removal. Freundlich model was applied to monitor the adsorption behavior. For 60 and 90 min of interaction, the data was well-fit by the equation, but for 30 min, the results were less satisfactory [44]. Table 1 lists information for utilizing plants from the Rosaceae, Paeoniaceae, and Malvaceae families.

Table 1. A summary on using plants from the Rosaceae, Paeoniaceae, and Malvaceae families.

Plant	Modification method	Adsorbate	%R	q (mg/g)	Opt. Cond.	Isotherm	Kinetic	The
Rose flower biomass		Hg (II), Cr (III), and Zn (II)		Chromium = 5.26, mercury = 7.62, and zinc = 4.07	100 ppm	Langmuir and Freundlich isotherms	Pseudo-second-order kinetics	
				chromium = 4.07, mercury = 6.76, and for zinc = 3.33	50 ppm			
Rose waste	Rose leaf coated with PPy (polypyrrole)	Pb (II)	RL = 56%, RL/PPy = 81%.		PH=8 Dosage=0.2 g/50 mL Stirring speed= 300 rpm Contact time=15 min	Freundlich model		
		Cd (II)	RL = 85%, RL/PPy = 92%.		PH=5 Dosage=0.2 g/50 mL stirring speed= 300 rpm contact time=45 min			
Alchemilla vulgaris leaves		MB	87.85%		The adsorbent concentration of 0.5 g/L and a dye concentration of 10 mg/L	Freundlich model	Pseudo-second-order kinetic	(ΔH_o) = 8.54 kJ/mol, (ΔS_o) = 12.283 J/mol (E_a) = 25.535 kJ/mol The adsorption p spontaneous
Paeonia ostii seed coats	Phosphoric acid-modified Paeonia ostii seed coats	Cu (II)		Exhibited a substantial four-fold increase when compared		Freundlich	Pseudo-second-order	Endothermic, spontar

	(PA-PSC)			to raw PSC			models	
Paeonia ostii seed coats	Iminodiacetic acid-functionalized Paeonia ostii seed coats (IDA-PSC)	Cu (II)		36.6	25°C	Langmuir models	Pseudo-second-order and	Spontaneous and end
Paeonia ostii seed coats		MB		368.2	25°C 0.8% (w/w) NaOH, liquid-solid ratio of 0.35 L g^{-1}, 50 min	Langmuir isotherm	Pseudo-second-order models	Endothermic, and spo
Hibiscus rosa-sinesis		MB	86%		dye concentration =10 mg L^{-1} pH= 6	Langmuir isotherm	Pseudo-first-order model	
Hibiscus cannabinus	Series of activation processes involving KOH treatment and carbonization	Safranin dye.			pH= 11 Adsorbent dosage = 0.2 g/L Initial dye concentration = 50 mg/L, 30 °C	Langmuir isotherm	Pseudo-second-order model	
Hibiscus Sabdariffa	Acid Activated Hibiscus Sabdariffa Nano Carbon (AHSNC)	Safranin dye				Langmuir and Freundlich isotherm models	Pseudo second-order model	
Leaf powder of		Removal of chromium from electroplating			60 min	Freundlich		

Hibiscus mutabilis		industry waste						

3-4 Asteraceae

Worldwide, the Asteraceae comprise more than 2500 species and 1600 genera, making it one of the largest collections of angiosperms. Among the most well-known members of this family are dandelion, chicory, artichoke, daisies, and lettuce. Medicinal and dietary uses of Asteraceae members have persisted throughout human history. It is worth noting that all of these species have high amounts of inulin, a naturally occurring polysaccharide with powerful prebiotic effects. Here, different types of phytochemicals, such as phenolic acids, polyphenols, triterpenes, and flavonoids, are responsible for these therapeutic effects. The antioxidant properties, positive effects on cell proliferation, and other characteristics made the arctiin stands out [45]. The following plants are examples of this family that were used for adsorption.

3.4.1. Sunflower

The sunflower, scientifically known as Helianthus annuus L., is a native North American plant that has become an important oilseed crop across the world. Originating with Native American civilizations, it was cultivated for its culinary and medicinal uses as well as its ceremonial use in body painting. A taxonomy is developed within the large genus Helianthus, which has 51 different species, including 14 annual and 37 perennial variants. Particularly important in sunflower breeding is the practice of interspecific hybridization. This becomes particularly relevant when the cultivated variety's genetic diversity reaches a point of depletion, necessitating the exploration of beneficial genetic

traits present in wild counterparts [46]. In adsorption, sunflower seed husk and other parts of the plant were intensively studied due to their abundance and remarkable results. The following sections describe different forms of utilizing this plant.

3.4.1.1. Synergizing with $ZnCl_2$

Sunflower seed husk biochar synthesized by a two-step process involving $ZnCl_2$ activation and hydrothermal carbonization (HZSF) was thoroughly investigated for its remarkable efficacy in adsorbing the antibiotic tetracycline (TC) from aqueous solutions [47]. Using a range of surface analysis methods, the physical and chemical characteristics of the HZSF biochar were thoroughly investigated. Importantly, compared to non-modified biochar (1.3 $m^2 \cdot g^{-1}$), HZSF exhibited a substantially improved specific surface area of 1578.3 $m^2 \cdot g^{-1}$, an increase of more than 1200 times. The enhanced surface area of HZSF is a direct result of its better capacity to adsorb TC. At 298 K for 24 h, the Langmuir isotherm model well represented the TC adsorption behavior on HZSF, showing an outstanding maximum adsorption capacity (q_{max}) of 673.0 $mg \cdot g^{-1}$. It was revealed that strong intermolecular interactions, monolayer adsorption, and chemical adsorption were all considered in this adsorption process. Also, the study investigated the kinetics; the best match was the pseudo-second-order kinetic model, meaning that the rate-limiting phase was chemisorption. Based on Raman spectroscopy, which showed a lower intensity ratio between the D and G bands (I_D/I_G ratios) for the HSF and HZSF compared to sunflower seed husk pyrolyzed at 700 °C (SF-700), indicating increased thermal stability and reduced carbon structure disorder. The characterization of the biochar in HZSF revealed a highly graphitized structure. N_2 adsorption-desorption

isotherms and X-ray diffraction (XRD) patterns both pointed to HZSF's improved pore structure, which supported the crystalline structure. With most pores ranging from 2 to 25 nm, HZSF had a pore size distribution that was ideal for TC adsorption.

Based on the results, HZSF is versatile. It can effectively adsorb TC across a broad pH range and it is resistant to the effectiveness of many ions and organic substances found in water. Moreover, the adsorption process was favorable even in real water matrices such as tap water and river water, suggesting the applicability of HZSF in water treatment scenarios. Furthermore, the biochar displayed impressive reusability over ten consecutive adsorption-desorption cycles, with a minor reduction in TC removal efficiency.

$ZnCl_2$ was also utilized by Vunain et al. when they studied the application of sunflower seed hull activated carbon (SSHAC) as an economical and effective adsorbent for the removal of catechol and resorcinol from aqueous solutions [25]. The sunflower seed hull served as the precursor to prepare AC through physicochemical activation using $ZnCl_2$. The activated carbon is thoroughly characterized using FTIR spectroscopy, Scanning Electron Microscopy with Energy Dispersive X-ray (SEM-EDX) analysis, XRD, BET analysis, and nitrogen adsorption isotherms. These analyses reveal that SSHAC possesses a highly porous structure with significant microporosity and mesoporosity, making it a promising adsorbent.

In batch experiments, the adsorption efficiency of SSHAC was examined under various conditions, including pH, initial adsorbate concentration, contact time, adsorbent dosage, and solution temperature. The Langmuir isotherm model effectively describes the equilibrium adsorption data, and the kinetics of the adsorption process follow a pseudo-

second-order model. The negative Gibbs free energy indicates the spontaneity of the adsorption, while the positive values of enthalpy assume an endothermic nature. The adsorption capacity increases with higher temperatures, reinforcing the potential application of SSHAC in endothermic adsorption processes. The maximum monolayer adsorption capacity was 271 mg/g for catechol and 250 mg/g for resorcinol, emphasizing the efficacy of SSHAC for adsorption.

The economic viability of SSHAC is highlighted by a cost estimate, demonstrating that the production cost of AC from sunflower seed hull is significantly lower (10 times higher) than commercially available AC. This economic advantage, coupled with the renewable and abundant nature of sunflower seed hulls, positions SSHAC as a cost-effective and sustainable adsorbent for water treatment.

3.4.1.2. Preparing Activated Carbon

In another approach, the activated carbon was synthesized from the sunflower straw. Here, sunflower straw-activated carbon (SSAC) was successfully fabricated through a one-step activation method utilizing H_3PO_4 as the activator [48]. Four types of SSAC, namely SSAC1, SSAC2, SSAC3, and SSAC4, were obtained with various impregnation ratios of SSAC into H_3PO_4, 1:1, 1:2, 1:3, and 1:5, respectively. The results illustrated that the impregnation ratio significantly influenced the structural properties of SSAC, affecting pore volume, specific surface area, and microporosity. SSAC3 exhibited the highest specific surface area (1,794.01 m^2/g), while SSAC4 showed the smallest microporosity (0.0527 cm^3/g) and the biggest pore volume (2.549 cm^3/g). Elemental analysis indicated that the use of H_3PO_4 as an activator removed oxygen-containing

functional groups on the sunflower straw surface. The SSACs showed favorable adsorption kinetics, with the pseudo-second-order model fitting the experimental data well. The Langmuir isotherm model described SSAC3 and SSAC4, while the Freundlich isotherm model was appropriate for SSAC1 and SSAC2. Thermodynamic analysis revealed that the adsorption process was spontaneous and endothermic. SSAC4, with an impregnation ratio of 1:5, presented the highest removal rate (97.73%) and maximum adsorption capacity (2,763.36 mg/g) for acid fuchsin at 303 K. This study highlighted the potential of SSAC as a green and active carbon material for treating dye-containing wastewater.

3.4.1.3. Incorporating NPs

Incorporating metal oxide nanomaterials is another approach to utilizing the husk, where many studies reported its validity. Hence, a study investigated a novel CuO-coated sunflower husk (CSFH) for the simultaneous adsorption of three antibiotics, namely: Levofloxacin (LEV), Meropenem (MER), and Tetracycline (TC), from aqueous solutions [24]. The CSFH demonstrated enhanced adsorption capacities for the antibiotics compared to uncoated sunflower husk. The SEM analysis revealed remarkable morphological changes in CSFH after adsorption, indicating the formation of smoother surfaces and the aggregation of separated particles. Energy-dispersive X-ray spectroscopy (EDS) confirmed the stability of CuO NPs on the CSFH surface. The XRD analyses indicated structural changes upon coating with CuO NPs, while the FTIR spectra suggested the presence of various functional groups involved in the adsorption process. The pH-dependent adsorption study revealed that the CSFH was most effective at pH 6

due to electrostatic attractions. Kinetic modeling suggested that the pseudo-second-order model best described the adsorption process. The Langmuir isotherm model fitted well with the data, indicating monolayer adsorption on CSFH. However, the maximum adsorption capacities were 62.24 mg/g for LEV, 131.83 mg/g for MER, and 96.95 mg/g for TC. The results highlight the potential of CSFH as an efficient adsorbent for removing antibiotic residues from wastewater.

Another study on using NPs was conducted utilizing nitrogenous silane modified with Helianthus annuus husk extract for the interfacial separation of concentrated mixed dyes from solution [49]. The hydrothermally synthesized silane NPs exhibit rapid and highly efficient adsorption capabilities, with a mechanism primarily based on electrostatic attraction between the positively charged silane NPs and the negatively charged dye molecules. The addition of H. annuus extract during synthesis enhances the surface area and pore volume of the NPs, contributing to increased dye removal capacity. XPS analysis reveals nitrogen-containing functionalities on the NP's surface responsible for binding dye. The study elucidates the mechanism of concentrated dye removal, emphasizing the role of increased surface area, dye binding capacity, and interfacial separation facilitated by the disruption of colloidal stability. For further illustration, the adsorption process is characterized by the Langmuir and Freundlich parameters. Results from zeta potential experiments show that dye binding destabilizes colloidal systems. Additionally, a bacterial viability experiment was performed to assess the treatment's environmental suitability, and the results indicate that there is minimal impact. Figure 2 shows that the removal of concentrated dye is orchestrated by the purposeful use of positively charged silane NPs. A solution containing positively charged soluble silane

NPs and negatively charged dye is mixed in the first step. The complex is quickly precipitated from the solution as a result of the electrostatic interaction between the negatively charged dye and the positively charged silane NPs. This could be considered a difficult but effective separation process that allows for the later removal of the settled insoluble silane nanoparticle/dye combination.

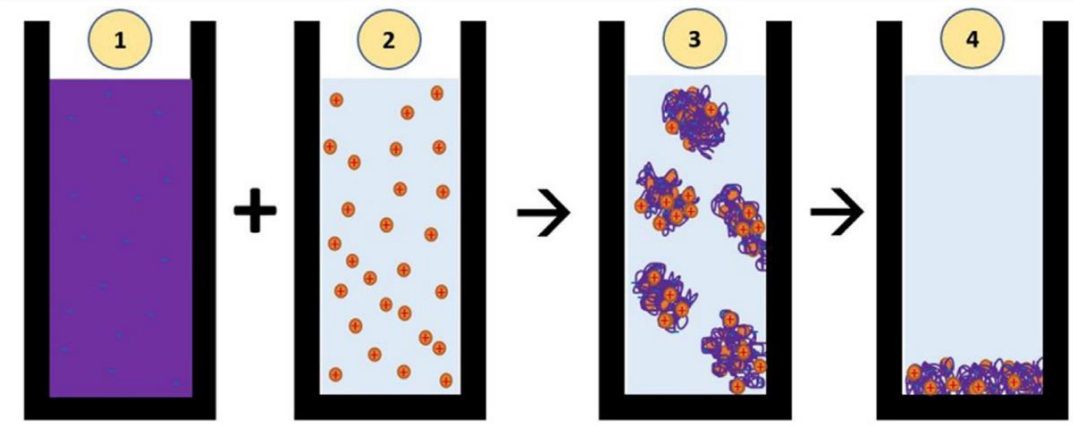

Figure 2. Removal of concentrated dye through the Interaction of negatively charged dye with positively charged silane nanoparticles. The process involves combining a mixed dye solution with a negative charge (1) with soluble silane nanoparticles possessing a positive charge (2). The positive charge on the silane nanoparticles attracts the negatively charged dye, resulting in the formation of a complex that precipitates from the solution (3). The settled insoluble silane nanoparticle/dye complex can then be removed in a subsequent stage (4). (Reprinted with permission from [49]. Copyright 2020; Elsevier publishing due to open access).

3.4.1.4. Use of roots

In a research by Srikantan et al. [50], the interaction between light and the adsorption dynamics of Reactive Red 120 dye by sunflower hairy roots is thoroughly investigated. Notably, light exposure affects the equilibrium and kinetics of dye adsorption in a root culture system. The study revealed that under a 16/8 h light/dark photoperiod, the

maximum adsorption capacity of the hairy roots experienced a remarkable six-fold increase, rising from 0.26 mg/g under complete darkness to 1.51 mg/g. To elucidate the adsorption process, the study employs a pseudo-first-order kinetic model; it demonstrated that Langmuir isotherm provides the most accurate description of the adsorption equilibrium. Additionally, FTIR analysis suggested that the dye undergoes structural changes, indicating potential degradation upon adsorption by the hairy roots.

The study proposed a strategy for dual-purpose application: alongside efficient dye removal, it also enhanced the production of alpha-tocopherol, a valuable antioxidant of industrial importance. The research findings underscored the profound impact of light on adsorption processes and raised the possibility of developing a cost-effective and environmentally friendly method for the tertiary treatment of textile dye effluents. Expanding the possible implications of this new technique, future research might concentrate on adjusting light intensity and photoperiod to enhance dye absorption and antioxidant synthesis in Helianthus annuus hairy roots.

In another investigation, the adsorption capacity exhibited by root exudates from sunflowers towards Cd (II) was explored [51]. The work described in detail the pH-dependent adsorption dynamics using a multi-technique approach that included a Cd ion-selective electrode, FTIR spectroscopy, and fluorescence spectroscopy. A maximum adsorption capacity of 150.8 mg/g was demonstrated in the experiments, with a pH of 7.0 being the most prominent. The physicochemical analysis of root exudates focused on active groups, with carboxyl groups having pKa values of 4.7 and phenolic and amino groups having pKa values of 9.2. Important components of the Cd (II) adsorption process included aliphatic and aromatic (C-H) groups, the amide III group, the C (=O)-O,

sulfonate groups, and others. Additionally, EEM fluorescence spectra, a type of fluorescence spectroscopy, provided more information. The existence of protein-like molecules engaging in Cd adsorption was suggested by two peaks, A and B, which correspond to Ex/Em values of 220/338 nm and 280/342 nm, respectively. The significant binding capacity of fluorescent components in root exudates to Cd (II) was highlighted by fluorescence quenching titration tests, which showed a dramatic drop in fluorescence intensity with increasing Cd (II) concentration. With conditional stability constants (log Ka) of 4.70 for peak A and 4.32 for peak B, the Stern-Volmer model characterized the quenching mechanism as a static process. In addition, the study investigated the pH effect on Cd binding capability and found that the process was pH-dependent, with 7.0 being the optimal pH for binding [51]. A maximum of 854.7 mmol g^{-1} of Cd and total organic compounds was bound by root exudates, as shown by the potentiometry measurements that demonstrated the significant complexation of Cd. The overall conditional stability constant (log K) was determined to be 5.13, indicating that root exudates had a strong affinity for Cd (II). The complex molecular interactions between root exudates and Cd (II) have the potential to affect phytoremediation efforts and the environment at large.

3.4.1.5. Chemically modified

In this section, the use of chemicals to modify the herbs is discussed. For instance, chemically treated Helianthus annuus flowers (SHC) were employed as an adsorbent to optimize the removal efficiency of Cr (VI) using the RSM [52]. The surface structure of SHC was meticulously examined through SEM coupled with EDX analysis, revealing

irregular cavities in the fibrous network, which enhance accessibility to Cr (VI). Batch mode experiments demonstrated a noteworthy adsorption capacity (q_e) of 7.2 mg/g. The study systematically assessed the impact of three crucial parameters, namely: pH of the solution (ranging from 2.0 to 7.0), initial Cr (VI) concentration (10–70 mg/L), and adsorbent dose (0.05–0.5 g/100 mL). The experimental design utilized the Box–Behnken model to determine the optimum pH, adsorbent dose, and initial Cr (VI) concentration as 2.0, 5.0 g/L, and 40 mg/L, respectively, resulting in a remarkable 90.8% removal efficiency under these conditions.

The study delves into the detailed analysis of the adsorbent using FT-IR, SEM, and EDX techniques. The SEM microscopic images reveal irregular cavities in the fibrous network, which are deemed beneficial for Cr (VI) accessibility. The EDX analysis provides direct evidence of the specific adsorption of chromium ions onto the adsorbents. Further exploration involves the application of Langmuir, Freundlich, and Dubinin–Radushkevich (D–R) isotherm models to interpret the equilibrium adsorption data. Among these, the Langmuir model exhibited a strong fit, with Q_0 and b values of 53.8 mg/g and 0.12 L/mg, respectively. The Freundlich model constants were determined as K_f (14.5 mg g^{-1}) and n (3.3 L mg^{-1}), while the D–R constants were found to be q_D (47.9 mg g^{-1}), B_D (0.363 mol^2 kJ^{-2}), and E_D (1.17 KJ mol^{-1}). The kinetic study employed pseudo-first-order and pseudo-second-order equations, with the latter proving more accurate in describing the adsorption of Cr (VI) ions. The RSM approach, with a quadratic equation model, was employed for optimization, taking into account the parameters' combined effects. The analysis of variance (ANOVA) indicated that the quadratic model was statistically significant for the adsorption process, where the

confirmation experiments were conducted under optimized conditions.

Another study aimed to assess the efficacy of sunflower waste, specifically sunflower stem, for the removal of Cr (VI) from aqueous solutions, investigating various process conditions [53]. Two distinct adsorbents were prepared through different pre-treatment methods: one involved boiling the sunflower stem waste (BSS), and the other utilized formaldehyde-treated sunflower stem waste (FSS). Batch experiments were systematically conducted, exploring the impact of solution pH, adsorbent dosage, initial Cr (VI) concentration, and contact time. The physicochemical properties and morphology of the adsorbents were analyzed using FT-IR spectroscopy and SEM, where SEM images show the difference in the prepared samples as shown in Figure 3. The results revealed that the removal efficiency of chromium was significantly influenced by the adsorbent's characteristics and the studied parameters. The maximum removal of Cr (VI) was observed at a pH of 2.0, with boiled sunflower stem absorbent exhibiting a removal efficiency of 81.7%, and formaldehyde-treated sunflower stem absorbent showing 76.5% removal at a 4.0 g/L adsorbent dose for dilute solutions. Isotherm models of Langmuir, Freundlich, and D–R were applied to describe the adsorption process, where the BSS was best described by Langmuir and D-R models, and the FSS was best described by the Freundlich model. The FT-IR spectra illustrated shifts in vibrational frequencies, suggesting the involvement of specific functional groups in the adsorption of Cr (VI) ions. SEM images displayed changes in the surface morphology of the adsorbents after Cr (VI) treatment. The study confirms that sunflower stem waste, particularly the boiled variant, could present an economical and environmentally sustainable method for removing pollutants.

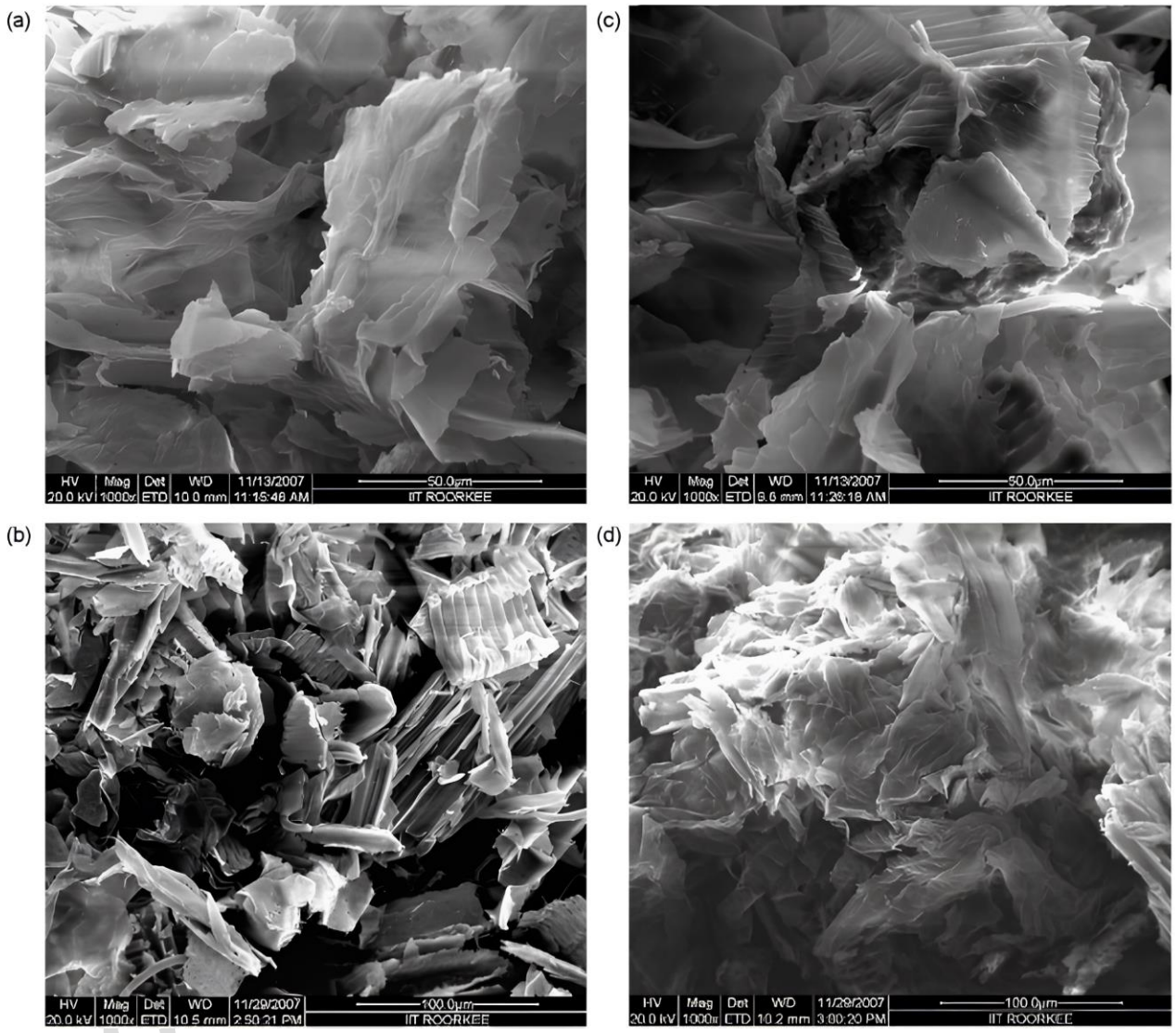

Figure 3. SEM images depicting various samples: (a) SEM images of untreated BSS, (b) SEM images of BSS loaded with Cr (VI), (c) SEM images of untreated FSS, and (d) SEM images of FSS loaded with Cr(VI) [53]. (Reprinted with permission from [53]. Copyright 2009; Elsevier publishing due to open access).

3.4.1.6. Plain plant

In this part, we will discuss the use of plain plants as adsorbents. Here, in an experimental study, the efficacy of SSH in removing Ni (II) ions from industrial wastewater was investigated and compared with zeolite [54]. The structural similarity

between SSH and zeolite prompted their interchangeable use in extracting Ni (II) ions from synthesized and real industrial wastewater. To investigate the industrial application of adsorbates, wastewater samples from two distinct companies, namely Pooshesh Loab and Rangin Poosheh located in Shiraz/ Iran, were collected. Then, batch adsorption experiments were conducted to optimize the adsorbent size, revealing that bulk-sized SSH exhibited a maximum adsorption rate of 76% under selected conditions. Morphological studies using SEM illustrated the porous structure of SSH, while FTIR spectroscopy highlighted changes in functional groups before and after the adsorption process. The study investigated the effects of adsorbent type, contact time, pH, and temperature on Ni (II) ion removal. Langmuir isotherm modeling was employed to analyze adsorption data, revealing favorable monolayer adsorption, and the thermodynamic parameters indicated the spontaneity and exothermic nature of the sorption process. Furthermore, the application of SSH in removing Ni (II) ions from industrial effluents was demonstrated, showing promising results compared to zeolite. Figure 4 shows a comparison of removal rates between the two adsorbates.

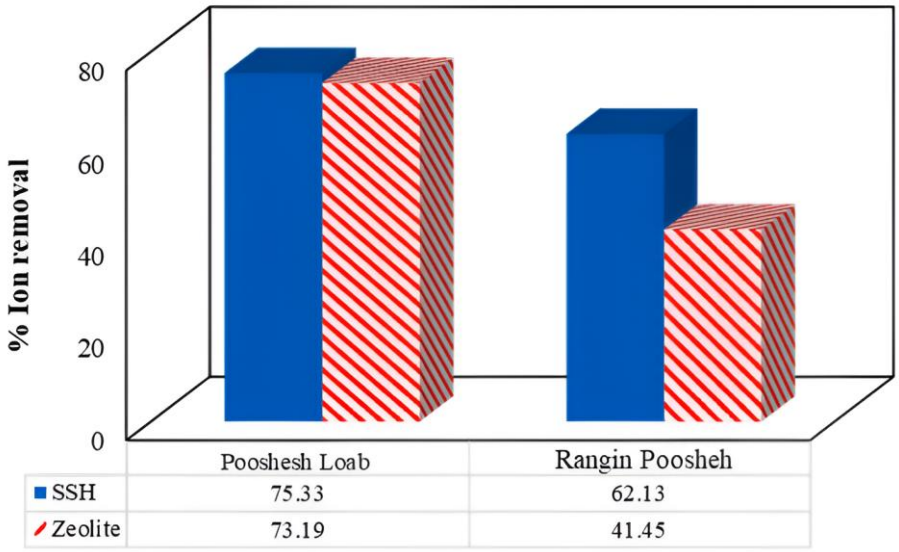

Figure 4. A comparison of the percentage of Ni(II) ion removal from industrial wastewater samples using SSH and Zeolite [54]. (Reprinted with permission from [54]. Copyright 2023; Elsevier publishing due to open access).

Another study investigated the efficacy of raw Helianthus annuus L. seed shells (HASS) as a natural adsorbent for the removal of Reactive Blue 221 (RB221) and Red X-5GN (RB14) dyes, which are representative of anionic and cationic dyes, respectively [55]. Optimal conditions for RB221 removal were observed at pH 2, achieving a treatment efficiency exceeding 90%, while BR14 exhibited optimal removal at pH 4 with a 97% efficiency. The appropriate adsorbent dosages were determined to be 4 g/L for RB221 and 10 g/L for BR14. The adsorption data were well-fitted to the pseudo-second-order kinetic model and the Langmuir isotherm for RB221, while the Freundlich isotherm was more suitable for BR14. The study revealed that the adsorption conditions varied significantly for each dye. Characterization of HASS through SEM and FTIR analyses illustrated the heterogeneous surface and diverse functional groups contributing to the adsorption process. Here, future studies could explore the performance of HASS in real

textile wastewater scenarios and consider continuous column studies for practical applications.

In the end, it is worth stating that sunflower-based adsorbents are recognized for their substantial surface area, making them adept to efficiently adsorbing diverse dye molecules at low cost [56]. It was found that the pH influences the adsorptive properties, underscoring its significant role in governing the surface charge of adsorbents and the ionization degree of dye molecules. The pH-dependent variation in adsorption capacity is thoroughly examined for different sunflower-based adsorbents, shedding light on their effectiveness in various pH ranges for different types of dyes. Desorption studies are considered a critical parameter for assessing the practical applicability of adsorbents at an industrial scale. The efficiency of regeneration is highlighted as a crucial aspect influencing operational costs and industrial feasibility. The comprehensive examination of thermodynamic studies explores parameters like enthalpy, change in standard free energy, and entropy. The positive values of enthalpy indicate the endothermic nature of the biosorption process, while thermodynamic parameters provide insights into the spontaneity and affinity of the adsorption. Table 2 shows a summary of using sunflower plant parts and waste for environmental remediation.

Table 2. A summary of using sunflower parts for environmental remediation

Plant/Modification	**Modification method**	**Adsorbate**	**R (%)**	**q (mg/g)**	**Opt. Cond.**	**Isotherm**	**Kinetic**	**Thermodynamic**	**Ref.**
Sunflower seed husk biochar	Prepared by a two-step process involving $ZnCl_2$	TC		673.0	298 K for 24 h	Langmuir isotherm model	Pseudo-second-order		[47]

	activation and hydrothermal carbonization (HZSF)						kinetic model		
sunflower seed hull activated carbon	Prepared through physicochemical activation using $ZnCl_2$	Catechol and resorcinol		271 for catechol and 250 for resorcinol		Langmuir isotherm model	Pseudo-second-order kinetic model	End othermic and spontaneous	[25]
Sunflower straw-activated carbon (SSAC)	Prepared through a one-step activation method using H_3PO_4 as the activator	Treating dye-containing wastewater	SSAC4, with an impregnation ratio of 1:5, exhibited the highest removal rate (97.73%)	2,763	303 K	Langmuir isotherm model described SSAC3 and SSAC4, while the Freundlich isotherm model was suitable for SSAC1 and SSAC2	Pseudo-second-order model	Spontaneous and endothermic	[48]
CuO-coated sunflower husk (CSFH)		Removing antibiotic residues from wastewater LEV, MER, and TC.		62.24 mg/g for LEV, 131.83 for MER, and 96. for TEC	PH 6	Langmuir isotherm model	Pseudo-second-order model		[24]
Sunflower hairy roots	Interaction between light and the adsorption dynamics	Red 120 dye		1.51		Langmuir isotherm	Pseudo-first-order model		[50]
Root exudates from	Root exudates from sunflowers towards			150.8	pH 7.0		Stern-Volmer		[51]

sunflowers	Cd (II)						model		
Helianthus annuus flowers (SHC)		Cr (VI)	90.8%	53.8	pH 2.0, adsorbent dose 5.0 g/L, initial Cr (VI) concentration 40 mg/L	Langmuir model			[52]
Sunflower stem	Different pre-treatment methods: one involved boiling the sunflower stem waste (BSS), and the other utilized formaldehyde treatment (FSS)	Cr (VI)	boiled sunflower stem = 81.7%, formaldehyde-treated sunflower stem = 76.5%		Dose = 4.0 g/L pH = 2				[53]
Sunflower seed husk (SSH) as		Ni(II)	76%			Langmuir isotherm		Spontaneity and exothermic	[54]
Raw Sunflower seed shells)(HASS		RB221	90%		pH = 2 Dose = 4 g/L	Langmuir isotherm	Pseudo-second-order kinetic		[55]
		RB14	97%		pH = 4 concentration = 10 g/L	Freundlich isotherm			

3.4.2. Marigold

Various species of Tagetes (Marigold) are cultivated globally for decorative reasons. In Eastern nations, these flowers are used either individually or in garlands for social and religious events. Consequently, beyond its ornamental role, Tagetes is cultivated as a viable crop. Its short cultivation duration makes it a convenient choice for multi-crop systems, allowing it to be rotated with other agricultural or horticultural crops. Additionally, it is often planted alongside other crops, such as tomatoes, to provide beneficial effects to the latter. Notably, Tagetes exhibits some resistance to saline and adverse environmental conditions [57]. In wastewater treatment, this plant was applied to remove dyes as will be discussed in the following section.

In a study by Bazan et al., carbonaceous adsorbents were successfully obtained from the residue after supercritical extraction of marigold, undergoing physical activation and subsequent testing for nitrogen dioxide (NO_2) and iodine adsorption. The research explored the influence of carbonization and activation temperatures on textural parameters, the acid-base character of the surface, and the sorption properties of the ACs. The resulting ACs exhibited a low-developed surface area ranging from 2 to 206 m^2/g. Elemental composition analysis revealed changes in carbon, nitrogen, sulfur, and ash content during carbonization and activation. For instance, sample M7A8, activated at 800°C, demonstrated a surface area of 125 m^2/g, with an ash content of 53.9%. Textural parameters indicated that activation at 800°C resulted in a more developed surface area and porous structure, influencing sorption capacities. The ACs exhibited notable acid-base properties, with a shift towards a strongly basic character due to carbonization and activation. Despite the modest textural parameters, the study demonstrated that the ACs

effectively adsorbed NO_2. The most effective adsorbent, sample M7A8, exhibited a sorption capacity of 29.2 mg/g in dry conditions and 66.7 mg/g in mixed-dry conditions [58]. Figure 5 shows the adsorption capacity of six samples, where M and A refer to the material and activation with CO_2, respectively; while 5, 7, and 8 mean 500, 700, and 800 °C, respectively.

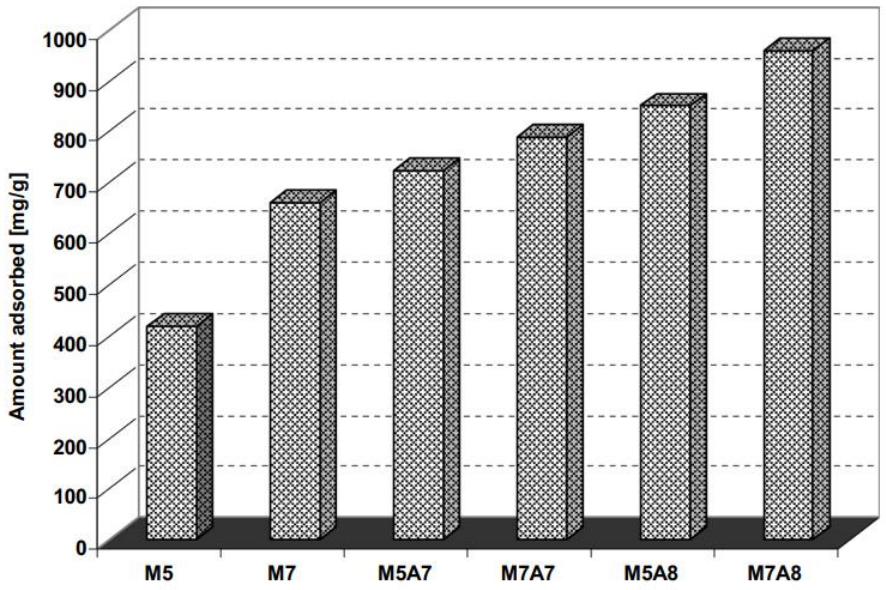

Figure 5. Adsorption of iodine on chars and activated carbons (mg/g) . It was used with permission from Springer Nature as the reference is under the terms of the Creative Commons CC BY license [58]. (Reprinted with permission from [58]. Copyright 2016; MDPI publishing due to open access).

In a more recent study from the same group, ACs derived from the residue of supercritical extraction of marigold were assessed for their efficacy in removing organic dyes from aqueous solutions. The activated carbons, produced through carbonization at different temperatures and subsequent activation, had predominant basic surface properties at a pH of 10.4 to 11.2. The highest adsorption capacity was observed in the sample activated at 800 °C, with values of 102.43 mg/g for methyl red, 139.72 mg/g for

methylene blue, 622.80 mg/g for malachite green, and 293.75 mg/g for crystal violet. The study revealed a dependence between adsorption capacities and various physicochemical properties of the ACs, including surface area, total pore volume, average pore diameter, basic functional group content, and mineral matter. As mentioned in the previous work, the activated carbons demonstrated competitive adsorption capacities despite relatively low specific surface areas compared to commercial adsorbents. Nevertheless, it is noteworthy that the examined AC samples exclusively feature basic functional groups on their surfaces. Consequently, electrostatic interactions between the adsorbent surface and adsorbate molecules are either absent or play a negligible role in the adsorption mechanism. It is plausible to hypothesize that the influence of π-π stacking interactions between the structure of ACs and dye molecules could be significant as illustrated in Figure 6. A comprehensive elucidation of the dye adsorption mechanism on the acquired carbon materials necessitates additional investigations. Hence, the study employed the Boehm method, Langmuir, Freundlich, and Temkin models for isotherm characterization, where the Langmuir model showed the best fit. The pseudo-second-order model was the best fit for kinetic analysis [59].

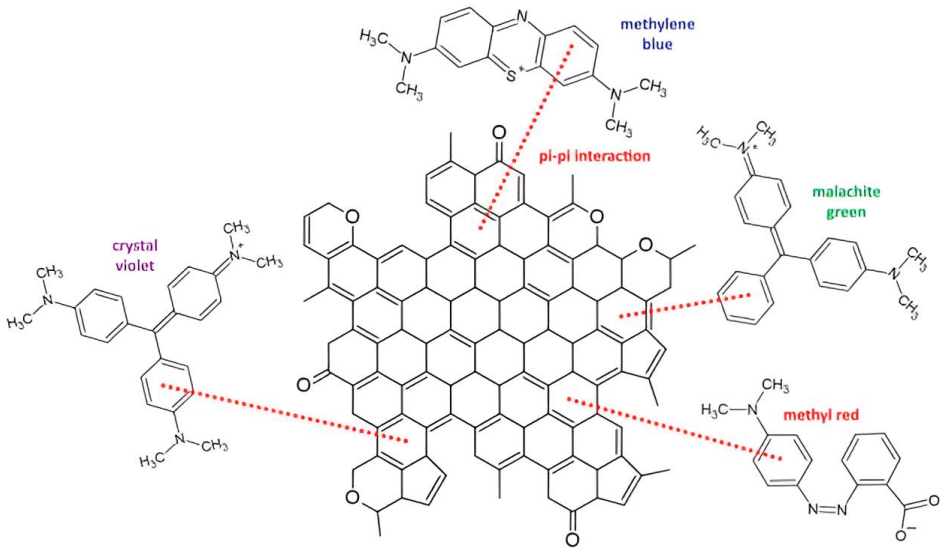

Figure 6. Organic dyes adsorption on activated carbons [59]. (Reprinted with permission from [59]. Copyright 2022; MDPI publishing due to open access).

In another study, marigold flower waste was employed as an adsorbent for the removal of cadmium (II) and chromium (VI) ions from aqueous solutions. The investigation encompassed a systematic analysis of influential parameters. The experimental results indicated a maximum removal efficiency of 83% for cadmium (II) at a contact time of 75 min and pH 5, while chromium (VI) exhibited a maximum removal efficiency of 96% at a contact time of 105 min and pH 3. The adsorption kinetics for both cadmium (II) and chromium (VI) were accurately described by the pseudo-second-order model, suggesting a boundary layer control mechanism as a rate-determining step. The Freundlich isotherm was found to fit the adsorption data well, with respective constants of 1.33 and 1.420 for cadmium (II) and 1.11 and 1.686 for chromium (VI). Thermodynamic analysis revealed negative values for Gibbs free energy, signifying the spontaneous nature of the adsorption process. Furthermore, negative values of enthalpy indicated an exothermic nature, and the stability of adsorbed species during the process

was affirmed by negative entropy values [60].

Another investigation repurposed waste marigold flowers as an adsorbent for the efficient removal of total arsenic ($As^{3+/5+}$) from contaminated water. The process involved the activation of marigold flower waste with iron salts (MG-Fe) and subsequent treatment with marigold plant extract (MG-Fe-Ex). The study systematically explored various factors influencing the adsorption process, including medium pH, temperature, pollutant concentration, reaction time, and adsorbent dose. With a dosage of 4 g/L, 20 mg/L of $As^{3+/5+}$, and a shaking rate of 120 rpm, MG-Fe-Ex achieved full elimination of $As^{3+/5+}$ at pH 8.0, 90 min, 30°C. Evidence from FTIR, EDS, dynamic light scattering (DLS), and XRD supported the involvement of iron oxides (Fe_2O_3 and Fe_3O_4) in MG-Fe-Ex. DLS showed that MG-Fe-Ex extracted As^{3+} and As^{5+} from water-based solutions better than other techniques due to its lower particle size. XRD analysis confirmed the crystalline nature of MG-Fe-Ex, revealing peaks from cellulose, hemicelluloses, γ-Fe_2O_3, and $Fe(OH)_2$. The EDS confirmed the presence of iron on the surfaces of MG-Fe and MG-Fe-Ex. The FTIR examination exposed the surface functional groups, including O-H, N-H, C-H, CH_2, CH_3, and Fe-O bonding. This research characterized the adsorption process using kinetic models (such as pseudo-first-order and pseudo-second-order) and isotherm models (such as Freundlich and Langmuir). The results were well-fit by the pseudo-first-order kinetic model, which points to a control mechanism involving the boundary layer. As^{3+} on MG-Fe-Ex showed multilayer coverage, but As^{5+} and $As^{3+/5+}$ on MG-Fe showed monolayer adsorption according to the Langmuir isotherm model fitting. According to the results of the thermodynamic study, the adsorption process is endothermic and occurs spontaneously [61].

Incorporating the NPs is another approach to modifying the plant. Here, a study presents an innovative and eco-friendly method for synthesizing CuO–ZnO–Carbon (CZC) nanocomposites (NCs) using marigold flower petals extract as a reducing agent and carbon source. The process involved filtration of fine powder from flower petals, supporting the growth of metal oxide nanorods/nanoparticles on the carbon surface. Subsequent modification with Cetyl Trimethyl Ammonium Bromide (CTAB) surfactant enhanced surface functionality, area, and positive charge density. CTAB-modified NCs demonstrate superior adsorption capacity for Cr(VI) and Congo red (CR) dye compared to unmodified NCs, particularly at neutral pH. The proposed adsorption mechanism involves electrostatic interactions between anionic Cr species and positively charged surface groups, with CTAB-modified NCs exhibiting enhanced adsorption due to increased positive charge density. Comparative analysis with other adsorbents reveals a significant improvement, with CTAB-CZC-300 NCs (prepared at 300 °C) achieving maximum adsorption capacities of 208.54 mg/g for Cr (VI) and 331.36 mg/g for CR dye at 30 ± 2 °C [62].

The suggested adsorption mechanism for Cr (VI) and CR dye on CZC-300 and CTAB-CZC-300 NCs is elucidated based on findings from FTIR and XPS analyses following the treatment of NCs with Cr(VI) and CR dye. The depicted reaction pathway is illustrated in Figure 7 When the solution pH is below 6, Cr forms anionic species ($HCrO_4^-$ and CrO_4^{2-}). Consequently, hydrophilic adsorption occurs through electrostatic interactions between these anionic Cr species and the positively charged surface of both NCs. The NC surface comprises carbon-containing functional groups, CuO, and ZnO, rendering it positively charged due to the influence of the point of zero charge (pH_{PZC}).

The CTAB-CZC-300 NCs exhibit a higher number of positive charge groups than CZC-300 NCs due to cationic modification with CTAB. Consequently, strong electrostatic interactions form between the cationic CTAB groups and the anionic Cr species, resulting in higher adsorption capacity for CTAB-CZC-300 NCs compared to unmodified CZC-300 NCs. Adsorption of Cr (III) species occurs in NCs post-adsorption due to the reduction of Cr (VI) by oxygen-containing functional groups.

A combination of hydrophilic and hydrophobic adsorption mechanisms for CR dye contributes to its adsorption onto CZC-300 and CTAB-CZC-300 NCs. Hydrophilic interactions involve electrostatic attraction between the anionic CR dye and the positively charged surface of both NCs. Additionally, hydrogen bonding occurs between CR dye and carbon-containing functional groups. In terms of hydrophobic adsorption, CZC-300 NCs, with carbon-containing functional groups, engage in hydrophobic interactions with π functional groups, including aromatic and aliphatic moieties of CR dye. CTAB-CZC-300 NCs offer more hydrophobic interaction sites due to the hydrocarbon chains of CTAB surfactant, resulting in enhanced hydrophobic interactions with the π functional groups of the dye. Consequently, CTAB-CZC-300 NCs exhibit superior adsorption capacity compared to CZC-300 NCs.

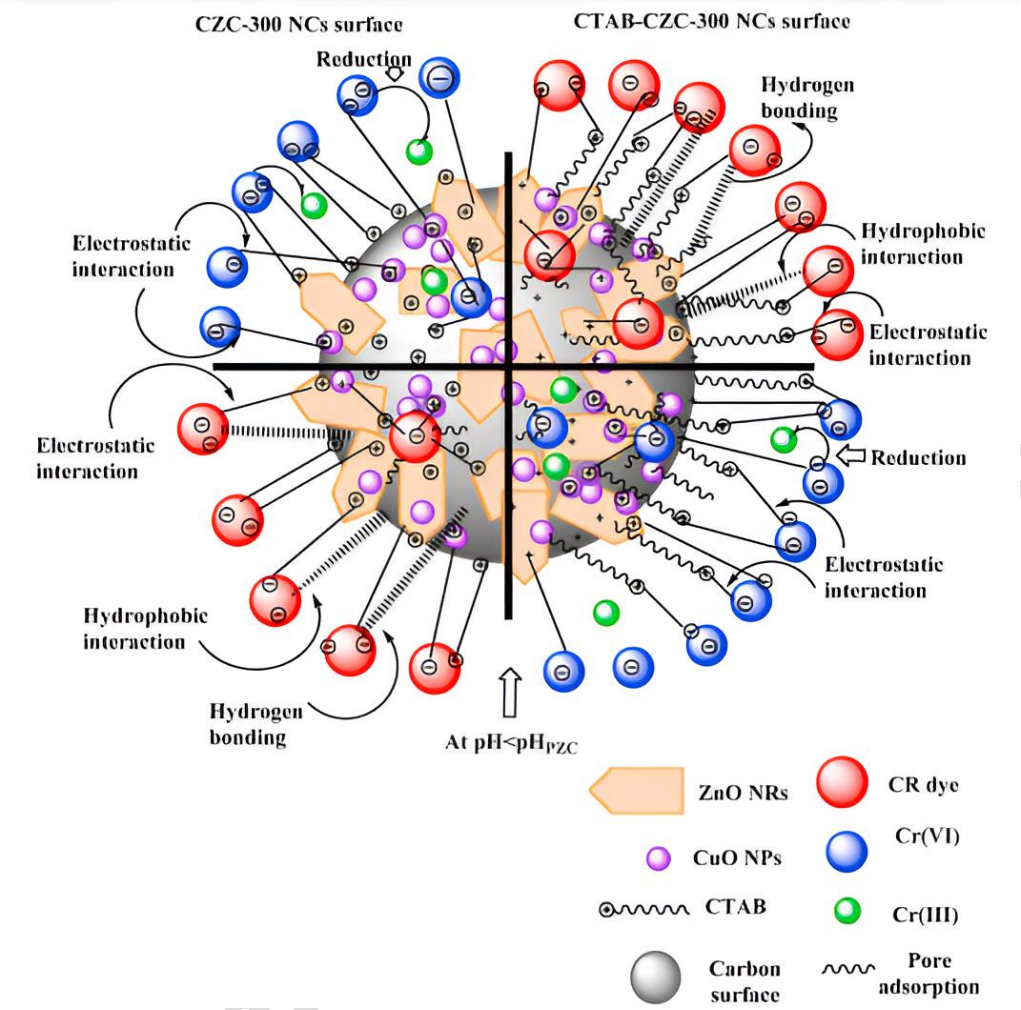

Figure 7. Possible reaction mechanism between the CZC-300 and CTAB-CZC-300 NCs with Cr (VI)/CR dye [62]. (Reprinted with permission from [62]. Copyright 2021; Elsevier publishing due to open access).

A separate study explored the potential of marigold flower waste as a sustainable source for charcoal production, subsequently employed as an effective adsorbent for Cu (II) metal ions in water remediation. Marigold flower charcoal (MFC) was characterized using SEM and EDS techniques, revealing a heterogeneous surface with available adsorption sites. SEM images before and after adsorption, along with EDS analysis, confirmed the successful adsorption of Cu (II) ions onto MFC. The adsorption data was well-fitted with the Temkin and D-R isotherm models, suggesting physical adsorption.

The study highlights the significance of flower waste utilization for water remediation, presenting MFC as a promising adsorbent with a maximum removal efficiency of 55.6%. The pseudo-second-order kinetic model was found to best describe the adsorption process [63]. There are further examples of utilizing the plants for phytoremediation, which is known for its green, pollution-free, and eco-friendly nature, emerged as a viable solution, where the significance of hyperaccumulative plants, critical in the phytoremediation process, is highlighted [64].

3.4.3. Chamomile

This plant was also investigated, where in a study, nano chamomile waste (NCW) was explored as a highly efficient and low-cost biosorbent for the rapid removal of heavy metal ions from natural water samples. Characterization analyses, including SEM, TEM, XRD, and FTIR, revealed morphological changes and the involvement of active functional groups, such as –OH and C=O, in metal adsorption. The biosorption mechanism was attributed to complexation adsorption, with gallic acid identified as a key ligand. Notably, NCW exhibited remarkable metal uptake capacities, reaching 621.6 mg/g for Pb (II), 163.9 mg/g for Cu(II), and 522.7 mg/g for Fe(III). The equilibrium data well-fitted with Langmuir and Freundlich models confirmed efficient adsorption. Kinetic studies revealed that the adsorption followed a pseudo-second-order mechanism with rapid equilibration within 30 seconds. The pH-dependent biosorption demonstrated optimum conditions at pH 5.5, 6.0, and 3.3 for Pb (II), Cu (II), and Fe (III), respectively. NCW, derived from waste, showcased superiority over other natural biosorbents, and its high removal efficiency (≥98%) was validated in diverse water samples [65].

We like to mention that we put the above-mentioned study to show an example of the potential use of chamomile although we don't agree with the NCW preparation method. The authors mentioned that they prepared the NCW via grounding and sieving the original powder using a domestic mill; while, to the best of our knowledge, the nano size can't be reached by this method.

3.4.4. Taraxacum

This plant was investigated by preparing biochar from Taraxacum mongolicum Hand-Mazz biomass that was modified with phosphorus (PLBC) and evaluated for As^{3+} removal from water. The study employed comprehensive characterization techniques, including SEM-EDS, TEM, FTIR, and XRD analyses, to elucidate the surface modifications and morphological changes in the biochar. SEM images revealed a crystalline and smooth structure of the base biochar, transitioning to an amorphous form after pyrolysis. Importantly, the P sorption during the loading process was confirmed by the presence of visible white amorphous particles on the PLBC surface.

Elemental mapping demonstrated a uniform distribution of major constituents (C, O, K, P, Ca, Fe) on the PLBC surface, affirming the successful P loading; Figure 8 shows the elemental analysis in the plain and modified biochar. TEM images further showcased the outstanding uniform layered structure of PLBC. FTIR spectra revealed significant changes in functional groups, with the disappearance of C–H and O–H stretches in PLBC, indicating the impact of pyrolysis and P loading. The presence of PO_4^{3-} stretches in PLBC FTIR spectra suggested successful phosphorus incorporation. XRD patterns unveiled alterations in mineralogy, with the disappearance of certain minerals in PLBC

and the emergence of new peaks, signifying the formation of novel mineral phases due to PO_4^{3-} ions binding with bridging cations. The detailed surface characterization provided crucial insights into the structural and chemical transformations induced by phosphorus loading. PLBC demonstrated superior efficiency in removing As^{3+} compared to plain biochar. Langmuir isotherm modeling yielded the best fit to the experimental data, suggesting a homogenous rate of adsorption with a maximum adsorption capacity of 30.76 mg/g for PLBC at pH 5. Adsorption kinetics, analyzed using pseudo-second-order modeling, indicated a contact time of 24 h for equilibrium, revealing the efficient and rapid removal of As^{3+} by PLBC. The adsorption mechanism was attributed to chemisorption, with the presence of P on the biochar surface playing a crucial role. Chemisorption involved the formation of bonds between PO_4^{3-} ions and the residual charge of ligand bridging cations, resulting in the sorption of PO_4^{3-} ions onto the biochar surface [66].

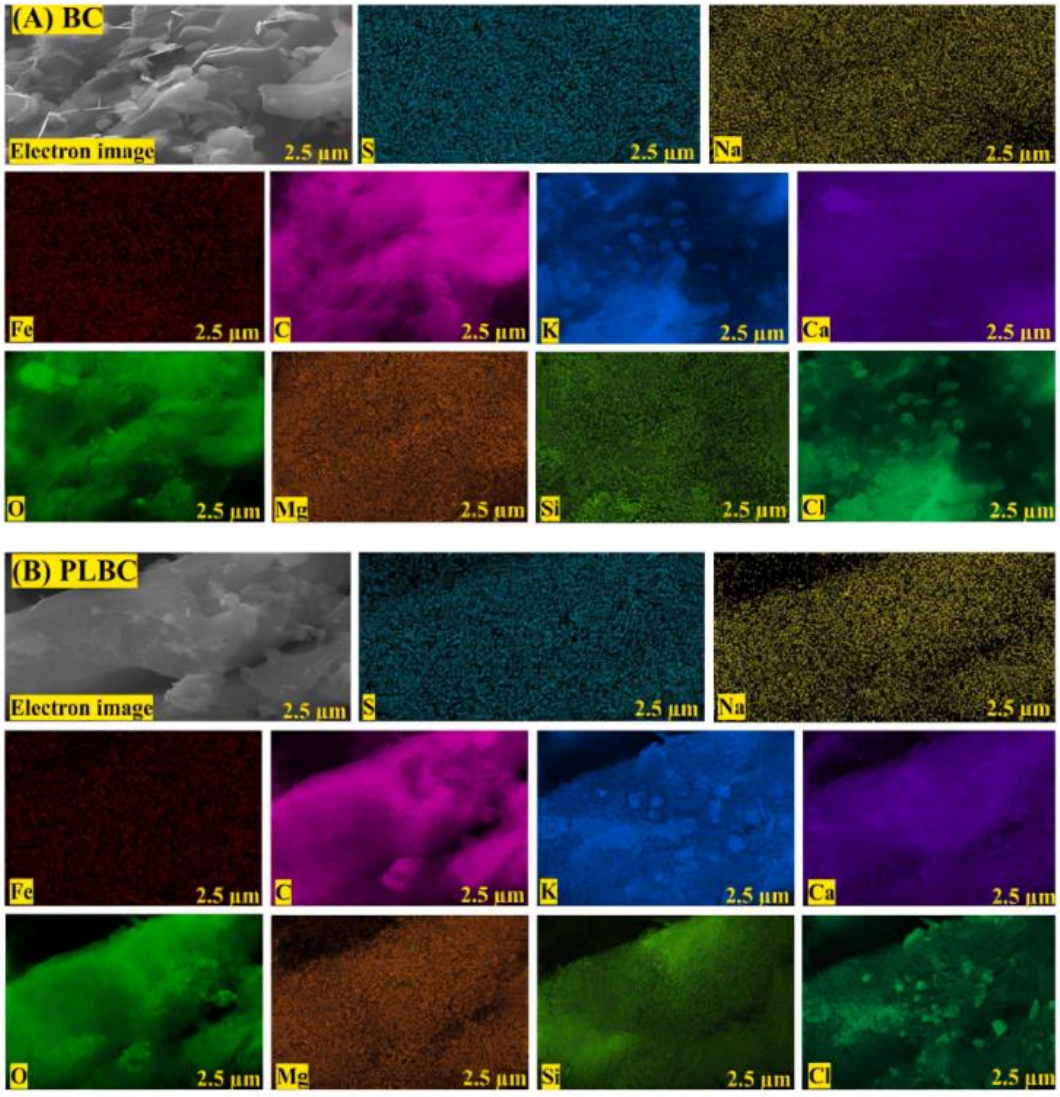

Figure 8. Elemental mappings of the homogenous dispersion of S, Na, Fe, C, K, Ca, O, Mg, Si, and Cl elements in plain biochar (A) and PLBC (B) [66]. (Reprinted with permission from [66]. Copyright 2021; Elsevier publishing due to open access).

In another study, the efficacy of dandelion (Taraxacum) root as a biosorbent (DRB) for the removal of strontium Sr(II)) and americium Am(III) ions from aqueous solutions was investigated. The adsorption kinetics revealed a rapid equilibrium within 90 min, and the adsorption process conformed well to the pseudo-second-order kinetic model. The Freundlich isotherm model, recognized for its applicability to heterogeneous

surfaces, excellently described the adsorption behavior, showcasing the heterogeneous nature of the DRB surface. Notably, at an optimal pH of approximately 6.0, the maximum adsorption capacities were determined to be 63.7 g kg^{-1} for Sr (II) and 80.6 g kg^{-1} for Am (III). The efficiency of DRB was prominently demonstrated, with 90% removal of Am (III) and 80% removal of Sr (II) achieved using merely 30 mg of biosorbent /1 mL of solution. Morphological changes in the DRB surface due to metal sorption were elucidated through SEM, revealing the structural alterations during the adsorption process. FTIR spectroscopy indicated the involvement of hydroxyl groups in inulin as the dominant metal complexing sites. The homogeneity of the DRB, as revealed by microscopic analysis, further supported its potential as an effective biosorbent. Thermal studies exhibited significant mass loss around 220 and 450 °C, suggesting the decomposition of organic components and the release of adsorbed metals. Crucially, the biosorbent's performance remained robust even in the presence of strong chelating agents, highlighting its resilience in complex environmental matrices. Desorption experiments underscored the recoverability of adsorbed metals, with desorption ratios of 0.331% for Sr (II) and 0.821% for Am (III) [67].

3.4.5. Nasturtium

This plant was applied in the biosorption of lead from aqueous solutions, where a natural absorbent of NoP (a powder derived from leached active ingredients) was utilized. This powder was explored for its performance and modeled using response surface methodology and central composite design. The NoP exhibited an irregular and porous structure, enhancing its biosorption capacity. The FTIR spectroscopy identified

functional groups (e.g., OH, CO, and carbonyl) on the NoP surface, rendering its suitability for interaction with contaminants. The response surface plots depicted interactive effects, revealing that 10 g/L of NoP yielded the optimal adsorption efficiency. The equilibrium data were well-described by Langmuir and Freundlich isotherm models, with the pseudo-second-order kinetics model fitting the biosorption process. Morphological changes observed through SEM and FTIR spectroscopy indicated the involvement of reactive sites in effective lead removal. Statistical analysis via analysis of variance confirmed the model's significance. Numerical optimization demonstrated the ability to achieve lead concentrations below the standard limit [68].

3.4.6. Yarrow

It is another Asteraceae plant, which was applied for adsorption purposes. Here, a study introduced a green and cost-effective method for synthesizing polyphenol-modified iron oxide nanoparticles (Aw-Fe_3O_4 NPs) using an aqueous extract of Achillea wilhelmsii C. Koch (Aw, a species of Yarrow) leaves. The NPs exhibited superior magnetism, crystalline structure, and high adsorption capacity for the cationic dye MB. The synthesis mechanism involved the hydrolysis and dehydratation of Fe^{2+} and Fe^{3+} salts in alkaline conditions, with polyphenolic compounds from Aw extract playing a crucial role in chelating ferric and ferrous hydroxide during nanoparticle nucleation. Adsorption studies revealed pH-responsive behavior, with maximum MB removal efficiency (73%) achieved at pH 11. The adsorption process was elucidated by electrostatic interactions, and the NPs followed the pseudo-second-order kinetic model and intraparticle diffusion model. The Aw-Fe_3O_4 NPs demonstrated efficient reusability over three cycles, proving their

potential for practical application in dye wastewater treatment [69]. Table 3 shows the results of using Asteraceae family plants (except sunflower) in environmental remediation.

Table 3. Performance of Asteraceae family (except sunflower) in polluted water treatment

Plant	**Modification method**	**Adsorbate**	**% R**	**q (mg/g)**	**Opt. Cond.**	**Isotherm**	**Kinetic**	**Thermodynamic**	**Ref.**
Marigold	Activated carbons derived from the residue of supercritical extraction of marigold	methyl red, methylene blue, malachite green, and crystal violet		methyl red = 102.43, methylene blue = 139.72, malachite green = 622.80, and crystal violet = 293.75	Activated at 800 °C	Langmuir model	Pseudo-second-order model		[59]
Waste marigold flower		Cd (II)	83 %		pH 5 75 min	Freundlich isotherm	Pseudo-second-order model	Exothermic nature and spontaneous	[60]
		Cr (VI)	96 %		pH 3 105 min				
Waste marigold flowers	Activation of marigold flower waste with iron salts (MG-Fe) and subsequent treatment	($As^{3+/5+}$)			pH 8.0 90 min 30°C Dose of 4 g/L 20 mg/L of $As^{3+/5+}$, Shaking	Langmuir isotherm model fitting indicated monolayer	Pseudo-first-order kinetic model	Endothermic and spontaneous	[61]

	with marigold plant extract (MG-Fe-Ex)				rate of 120 rpm	adsorption for As^{5+} on MG-Fe-Ex and $As^{3+/5+}$ on MG-Fe, while Freundlich isotherm revealed multilayer coverage for As^{3+} on MG-Fe-Ex			
Marigold flower petals extract	Filtration of fine powder from flower petals, supporting the growth of metal oxides nanorods/nanoparticles on the carbon surface.	Cr(VI)		208.54					[62]
		CR dye		331.36					
Marigold flower		Cu (II)	55.6 %			Temkin and Dubinin	Pseudo second-order		[63]

waste						- Radushkevich isotherm models	kinetic model		
Nano chamomile waste (NCW)		Pb(II) Cu(II) Fe(III)	98 %	Pb(II) = 621.6, Cu(II) = 163.9, Fe(III)= 522.7	PH Pb(II) = 5.5, Cu(II) = 6.0, and Fe(III) = 3.3	Langmuir and Freundlich models	Pseudo-second-order kinetic		[65]
Taraxacum mongolicum Hand-Mazz biomass	A phosphorus modified biochar (PLBC) synthesized from Taraxacum mongolicum Hand-Mazz biomass	As^{3+}		30.76	pH = 5 contact time of = 24 h	Langmuir isotherm model	Pseudo-second-order model		[66]
Dandelion (Taraxacum) root (DRB)		Sr(II))	80 %	63.7	90 min pH 6 30 mg/ml	Freundlich isotherm model	Pseudo-second-order kinetic model.		[67]
		Am(III)	90 %	80.6					
Nasturtium	Natural absorbent of NoP (a powder	Pb^{2+}			Dose = 10	Langmuir and Freundlich	Pseudo-second-order		[68]

	derived from leached active ingredients					isotherm models	kinetics model		
Achillea wilhelmsii C. Koch (Aw, a species of Yarrow) leaves	Synthesizing polyphenol-modified iron oxide nanoparticles (Aw-Fe_3O_4 NPs) using an aqueous extract of Achillea wilhelmsii C. Koch (Aw, a species of Yarrow) leaves	MB	73 %		pH 11		Pseudo-second-order kinetic model		[69]

4. Adsorption Mechanisms

In this study, a diverse array of adsorption mechanisms was employed by herbaceous plant-based adsorbents, each contributing uniquely to the removal of pollutants. For instance, the adsorption of HMs on rose biomass was found to follow both Langmuir and Freundlich isotherms, indicating the presence of multiple adsorption sites and mechanisms. The process best described by pseudo-second-order kinetics, which suggests a rate-limiting step [27]. While the conductive properties of polypyrrole were primarily governed by a p-type (bipolaron) process, where electron hopping across

polymer chains and ion movement within the polymer network play crucial roles [29]. Additionally, the adsorption of Pb (II) ions by a composite material was facilitated by an electron-sharing mechanism involving nitrogen atoms in the polymer structure [30]. Other studies showed that the interaction between the adsorbents and pollutants was influenced by various mechanisms, including hydrogen bonds, Van der Waals forces, and ion exchange, which contribute to the complexity and effectiveness of the adsorption process [35].

Hydrothermally synthesized silane NPs demonstrate a mechanism based on electrostatic attraction between the positively charged NPs and negatively charged dye molecules, enhanced by increased surface area and pore volume resulting from the inclusion of Helianthus annuus extract [49]. The quenching mechanism in the Stern-Volmer model was also identified as a static process, with pH-dependent binding of Cd ions, optimal at pH 7.0 [51]. While the adsorption of arsenic species on modified biochar was described by a combination of pseudo-first-order kinetics and Langmuir isotherm, indicating monolayer adsorption and an endothermic, spontaneous process [61]. Finally, the adsorption of Congo Red dye onto NCs involved both hydrophilic interactions, such as electrostatic attraction and hydrogen bonding, and hydrophobic interactions with carbon-containing functional groups and π functional groups, with enhanced adsorption capacity observed in surfactant-modified NCs [62]. Here, all of the adsorption mechanisms highlight the synergistic effects of various physical and chemical interactions, including chemisorption, electrostatic attraction, and hydrophobic interactions, in achieving effective pollutant removal.

5. Conclusion

This review highlights the many uses of herbaceous plants, specifically focusing on families like Rosaceae, Paeoniaceae, Malvaceae, and Asteraceae. The study emphasizes the efficiency, economic viability, and environmental sustainability of herbaceous plants, particularly sunflower-based materials, for water treatment. The study explores the adsorption properties of several plant components, such as seed husks, straws, roots, and raw plant matter, highlighting the adaptability and efficiency of sunflower (Helianthus annuus L.) as a long-term, environmentally friendly adsorbent. Chemical modification, activation with metal oxide nanoparticles, and usage of root systems are some of the approaches thoroughly examined in the inquiry, which highlights the potential of biomass-based products in tackling environmental concerns associated with water pollution. The work sheds light on adsorption mechanisms, influencing variables, and enhanced characterization techniques; it also highlights the economic feasibility of materials derived from herbs.

In addition, the review showcased the extensive use of some herbaceous plants, such as marigolds and sunflowers, in adsorption procedures for environmental cleanup, compared to other plants. Also, very high adsorption performance was achieved using activated carbon made from sunflower waste, which reached 2,763.36 mg/g when the AC was applied to remove acid fuchsin dye. Taken as a whole, the results highlight the promise of plant-based materials as sustainable and economical adsorbents for a wide range of water treatment applications involving the removal of pollutants. To solve urgent worldwide water problems, this work opens the door to more research and use of herbaceous plants, particularly sunflowers, in water remediation technology development

that is both practical and sustainable.

6. **References**

[1] Ahmed AU, Ibraheem H, Kadhom M, Rashad AA, Al-Dahhan WH, Bufaroosha M. et al. Modified PVC as adsorbent for methyl orange dye removable. 2022; 020006. https://doi.org/10.1063/5.0093582.

[2] Ismail Z, Go YI. Fog-to-water for water scarcity in climate-change hazards hotspots: pilot study in southeast asia. Global Challeng. 2021;5(5): 2000036. https://doi.org/10.1002/gch2.202000036.

[3] Droogers P, Immerzeel WW, Terink W, Hoogeveen J, Bierkens MFP, van Beek LPH, et al. Water resources trends in Middle East and North Africa towards 2050. Hydrol Earth Syst Sci. 2012; 16:3101–14. https://doi.org/10.5194/hess-16-3101-2012.

[4] Salih SS, Mohammed HN, Abdullah GH, Kadhom M, Ghosh TK. Simultaneous removal of Cu(II), Cd(II), and industrial dye onto a composite chitosan biosorbent. J Polym Environ. 2020; 28:354-65. https://doi.org/10.1007/s10924-019-01612-x.

[5] Salih SS, Mahdi A, Kadhom M, Ghosh TK. Competitive adsorption of As(III) and As(V) onto chitosan/diatomaceous earth adsorbent. J Environ Chem Eng. 2019; 7:103407. https://doi.org/10.1016/j.jece.2019.103407.

[6] Jawad AH, Kadhum AM, Ngoh YS. Applicability of dragon fruit (Hylocereus polyrhizus) peels as low-cost biosorbent for adsorption of methylene blue from aqueous solution: kinetics, equilibrium and thermodynamics studies. Desalination Water Treat. 2018; 109:231-40. https://doi.org/10.5004/dwt.2018.21976.

[7] Adil H, Hussain Z, Kadhom M, Yousif E. Adsorptive removal of safranin-O dye from

aqueous solutions using carrot seed, 2022, 040011. https://doi.org/10.1063/5.0121105.

[8] Salih SS, Kadhom M, Shihab MA, Ghosh TK. Competitive adsorption of Pb(II) and phenol onto modified chitosan/vermiculite adsorbents. J Polym Environ. 2022;30:4238-51. https://doi.org/10.1007/s10924-022-02515-0.

[9] Boakye P, Ohemeng-Boahen G, Darkwah L, Sokama-Neuyam YA, Appiah-Effah E, Oduro-Kwarteng S, et al. Waste biomass and biomaterials adsorbents for wastewater treatment. Green Energy Environ Technol. 2022;2022:1-25. https://doi.org/10.5772/geet.05.

[10] Moussavi G, Mahmoudi M. Removal of azo and anthraquinone reactive dyes from industrial wastewaters using MgO nanoparticles. J Hazard Mater. 2009; 168:806-12. https://doi.org/10.1016/j.jhazmat.2009.02.097.

[11] Schweitzer L, Noblet J. Water contamination and pollution. Green Chemistry, Elsevier; 2018; 261-90. https://doi.org/10.1016/B978-0-12-809270-5.00011-X.

[12] Jacob JM, Karthik C, Saratale RG, Kumar SS, Prabakar D, Kadirvelu K, et al. Biological approaches to tackle heavy metal pollution: A survey of literature. J Environ Manage. 2018; 217:56-70. https://doi.org/10.1016/j.jenvman.2018.03.077.

[13] Mani S, Chowdhary P, Bharagava RN. Textile wastewater dyes: toxicity profile and treatment approaches. emerging and eco-friendly approaches for waste management, Singapore: Springer Singapore; 2019; 219-44. https://doi.org/10.1007/978-981-10-8669-4_11.

[14] Gupta VK, Suhas. Application of low-cost adsorbents for dye removal – A review. J Environ Manage. 2009; 90:2313-42. https://doi.org/10.1016/j.jenvman.2008.11.017.

[15] Kadhom M, Albayati N, Alalwan H, Al-Furaiji M. Removal of dyes by agricultural

waste. Sustain Chem Pharm. 2020; 16: 100259. https://doi.org/10.1016/j.scp.2020.100259.

[16] Al-Ghouti MA, Sweleh AO. Optimizing textile dye removal by activated carbon prepared from olive stones. Environ Technol Innov. 2019; 16:100488. https://doi.org/10.1016/j.eti.2019.100488.

[17] Karadag D, Akgul E, Tok S, Erturk F, Kaya MA, Turan M. Basic and Reactive Dye Removal Using Natural and Modified Zeolites. J Chem Eng Data. 2007; 52:2436-41. https://doi.org/10.1021/je7003726.

[18] Kadhom M, Kalash K, Al-Furaiji M. Performance of 2D MXene as an adsorbent for malachite green removal. Chemosphere. 2022; 290:133256. https://doi.org/10.1016/j.chemosphere.2021.133256.

[19] Karadag D, Akgul E, Tok S, Erturk F, Kaya MA, Turan M. Basic and Reactive Dye Removal Using Natural and Modified Zeolites. J Chem Eng Data. 2007; 52:2436-41. https://doi.org/10.1021/je7003726.

[20] Alalwan HA, Kadhom MA, Alminshid AH. Removal of heavy metals from wastewater using agricultural byproducts. J Water Supply: Res Technol-AQUA 2020; 69:99-112. https://doi.org/10.2166/aqua.2020.133.

[21] Decocq G, Andrieu E, Brunet J, Chabrerie O, De Frenne P, De Smedt P, et al. Ecosystem Services from Small Forest Patches in Agricultural Landscapes. Current Forestry Rep. 2016;2:30–44. https://doi.org/10.1007/s40725-016-0028-x.

[22] De Leijster V, Santos MJ, Wassen MJ, Ramos-Font ME, Robles AB, Díaz M, et al. Agroecological management improves ecosystem services in almond orchards within one year. Ecosyst Serv. 2019; 38:100948. https://doi.org/10.1016/j.ecoser.2019.100948.

[23] Lüscher A, Barkaoui K, Finn JA, Suter D, Suter M, Volaire F. Using plant diversity to reduce vulnerability and increase drought resilience of permanent and sown productive grasslands. Grass Forage Sci. 2022;77:235-46. https://doi.org/10.1111/gfs.12578.

[24] Ibrahim AM, Ali A, Shaban M, Rashid Hasan Y, J. M Ridha M, A. Hussein H, M. Abed K, et al. Simultaneous adsorption of ternary antibiotics (levofloxacin, meropenem, and tetracycline) by sunflower husk coated with copper oxide nanoparticles. J Ecolog Eng. 2022; 23:30-42. https://doi.org/10.12911/22998993/147806.

[25] Vunain E, Houndedjihou D, Monjerezi M, Muleja AA, Kodom B. Adsorption, Kinetics and equilibrium studies on removal of catechol and resorcinol from aqueous solution using low-cost activated carbon prepared from sunflower (helianthus annuus) seed hull residues. Water Air Soil Pollut. 2018; 229:366. https://doi.org/10.1007/s11270-018-3993-9.

[26] Karaboyaci M. Recycling of rose wastes for use in natural plant dye and industrial applications. J Text Instit. 2014; 14:1-7. https://doi.org/10.1080/00405000.2013.876153.

[27] Aman A, Ahmed D, Asad N, Masih R, Abd ur Rahman HM. Rose biomass as a potential biosorbent to remove chromium, mercury and zinc from contaminated waters. Intern J Environ Stud. 2018; 75:774-87. https://doi.org/10.1080/00207233.2018.1429130.

[28] Canoluk C, Gursoy S Sen. Chemical modification of rose leaf with polypyrrole for the removal of Pb (II) and Cd (II) from aqueous solution. J Macromol Sci Part A. 2017; 54:782-90. https://doi.org/10.1080/10601325.2017.1336722.

[29] Pelto J, Haimi S, Puukilainen E, Whitten PG, Spinks GM, Bahrami-Samani M, et al. Electroactivity and biocompatibility of polypyrrole-hyaluronic acid multi-walled carbon nanotube composite. J Biomed Mater Res A. 2010; 93A(3): 1056-1067.

https://doi.org/10.1002/jbm.a.32603.

[30] Tavallali H, Malekzadeh H, Karimi MA, Payehghadr M, Deilamy-Rad G, Tabandeh M. Chemically modified multiwalled carbon nanotubes as efficient and selective sorbent for separation and preconcentration of trace amount of Co(II), Cd(II), Pb(II), and Pd(II). Arabian J Chem. 2019;12:1487-95. https://doi.org/10.1016/j.arabjc.2014.10.034.

[31] Reçber Z. Adsorption of methylene blue onto spental chemilla vulgaris leaves: characterization, isotherms, kinetic and thermodynamic studies. Inter J Environ Sci Technol. 2022; 19:4803-14. https://doi.org/10.1007/s13762-022-04053-7.

[32] Tamura M. Paeoniaceae. Flowering Plants Eudicots, Berlin, Heidelberg: Springer Berlin Heidelberg; 2007; 265-9. https://doi.org/10.1007/978-3-540-32219-1_34.

[33] Liu Q, Han R, Qu L, Ren B. Enhanced adsorption of copper ions by phosphoric acid-modified Paeonia ostii seed coats. Environ Sci Poll Res. 2020; 27:43906-16. https://doi.org/10.1007/s11356-020-10296-z.

[34] Liu Q, Qu L, Ren B. Effective removal of copper ions from aqueous solution by iminodiacetic acid-functionalized *Paeonia ostii* seed coats. J Dispers Sci Technol. 2020; 41:1126-35. https://doi.org/10.1080/01932691.2019.1614457.

[35] Liu Q, Li T, Zhang S, Qu L, Ren B. Optimization and evaluation of alkali-pretreated paeonia ostii seed coats as adsorbent for the removal of Mb from aqueous solution. Polish J Chem Technol. 2018; 20:29–-36. https://doi.org/10.2478/pjct-2018-0035.

[36] Petrovska B. Historical review of medicinal plants′ usage. Pharmacogn Rev 2012; 6:1. https://doi.org/10.4103/0973-7847.95849.

[37] Boy HIA, Rutilla AJH, Santos KA, Ty AMT, Yu AI, Mahboob T, et al. Recommended medicinal plants as source of natural products: A review. Digital Chinese Medicine.

2018; 1:131-42. https://doi.org/10.1016/S2589-3777(19)30018-7.

[38] Riaz G, Chopra R. A review on phytochemistry and therapeutic uses of Hibiscus sabdariffa L. Biomed Pharmacot. 2018; 102:575-86. https://doi.org/10.1016/j.biopha.2018.03.023.

[39] McKay DL, Chen CYO, Saltzman E, Blumberg JB. Hibiscus Sabdariffa L. Tea (tisane) lowers blood pressure in prehypertensive and mildly hypertensive adults. J Nutr. 2010; 140:298-303. https://doi.org/10.3945/jn.109.115097.

[40] Kaur N, Kaushal J, Mahajan P. Phytoremediation potential of hibiscus rosa-sinesis for removal of methylene blue dye and its kinetic, adsorption studies in aquatic system. Asian J Chem 2022; 34:2710-6. https://doi.org/10.14233/ajchem.2022.23906.

[41] Raja YS, Samsudin MFR, Sufian S. Development of the low-cost and green hibiscus cannabinus bioadsorbent for the removal of dye in wastewater. Arab J Sci Eng. 2021; 46:6349-58. https://doi.org/10.1007/s13369-020-05066-5.

[42] Manivannan P, Arivoli Thiru Vi Ka S, Raja M. Isotherm analysis on the removal of safranin dye using acid activated hibiscus sabdariffa stem nano carbon. Res J Chem Environ. 2019; 23(9):94-100.

[43] Hoong HNJ, Ismail N. Removal of dye in wastewater by adsorption-coagulation combined system with *Hibiscus sabdariffa* as the coagulant. MATEC Web of Conferences 2018; 152:01008. https://doi.org/10.1051/matecconf/201815201008.

[44] Murali M. An international quarterly scientific journal some studies on the removal of chromium from electroplating Iindustry waste by the leaf powder of Hibiscus mutabilis. Nat Envi Pol Tech. 2016;15:657-60.

[45] Rolnik A, Olas B. The plants of the asteraceae family as agents in the protection of

human health. Int J Mol Sci. 2021; 22:3009. https://doi.org/10.3390/ijms22063009.

[46] Kaya Y, Jocic S, Miladinovic D. Sunflower. Technological innovations in major world oil crops, Volume 1, New York, NY: Springer New York; 2012, p. 85–129. https://doi.org/10.1007/978-1-4614-0356-2_4.

[47] Nguyen TB, Nguyen KT, Chen WH, Chen CW, Bui XT, Patel AK, et al. Hydrothermal and pyrolytic conversion of sunflower seed husk into novel porous biochar for efficient adsorption of tetracycline. Bioresour Technol. 2023; 373:128711. https://doi.org/10.1016/j.biortech.2023.128711.

[48] Zhao W, Chen L, Jiao Y. Preparation of activated carbon from sunflower straw through H3PO4 activation and its application for acid fuchsin dye adsorption. Water Sci Eng. 2023; 16:192-202. https://doi.org/10.1016/j.wse.2023.02.002.

[49] Truskewycz A, Taha M, Jampaiah D, Shukla R, Ball AS, Cole I. Interfacial separation of concentrated dye mixtures from solution with environmentally compatible nitrogenous-silane nanoparticles modified with Helianthus annuus husk extract. J Colloid Interface Sci. 2020; 560:825-37. https://doi.org/10.1016/j.jcis.2019.10.108.

[50] Srikantan C, Suraishkumar GK, Srivastava S. Effect of light on the kinetics and equilibrium of the textile dye (Reactive Red 120) adsorption by Helianthus annuus hairy roots. Bioresour Technol. 2018; 257:84-91. https://doi.org/10.1016/j.biortech.2018.02.075.

[51] Yang J, Pan X. Root exudates from sunflower (*Helianthus annuus* L.) show a strong adsorption ability toward Cd(II). J Plant Interact. 2013; 8:263-70. https://doi.org/10.1080/17429145.2012.737030.

[52] Jain M, Garg VK, Kadirvelu K. Investigation of Cr(VI) adsorption onto chemically

treated Helianthus annuus: optimization using response surface methodology. Bioresour Technol. 2011;102:600-5. https://doi.org/10.1016/j.biortech.2010.08.001.

[53] Jain M, Garg VK, Kadirvelu K. Chromium(VI) removal from aqueous system using Helianthus annuus (sunflower) stem waste. J Hazard Mater. 2009;162:365–72. https://doi.org/10.1016/j.jhazmat.2008.05.048.

[54] Tadayon Y, Bahrololoom ME, Javadpour S. An experimental study of sunflower seed husk and zeolite as adsorbents of Ni(II) ion from industrial wastewater. Water Resour Ind. 2023; 30:100214. https://doi.org/10.1016/j.wri.2023.100214.

[55] Cesur Özcan EN, Gürel L. A comparison for the removal of two different textile dyes by raw Helianthus annuus L. seed shells. Inter J Enviro Sci Technol. 2023; 20:6791-804. https://doi.org/10.1007/s13762-022-04729-0.

[56] Anastopoulos I, Giannopoulos G, Islam A, Ighalo JO, Iwuchukwu FU, Pashalidis I, et al. Potential environmental applications of Helianthus annuus (sunflower) residue-based adsorbents for dye removal in (waste)waters. Biomass-Derived Materials for Environmental Applications, Elsevier; 2022, 307-18. https://doi.org/10.1016/B978-0-323-91914-2.00008-8.

[57] Vasudevan P, Kashyap S, Sharma S. Tagetes: a multipurpose plant. Bioresour Technol. 1997; 62:29-35. https://doi.org/10.1016/S0960-8524(97)00101-6.

[58] Bazan A, Nowicki P, Pietrzak R. Removal of NO_2 by carbonaceous adsorbents obtained from residue after supercritical extraction of marigold. Adsorption. 2016; 22:465-71. https://doi.org/10.1007/s10450-015-9709-1.

[59] Bazan-Wozniak A, Wolski R, Paluch D, Nowicki P, Pietrzak R. Removal of organic dyes from aqueous solutions by activated carbons prepared from residue of supercritical

extraction of marigold. Materials. 2022; 15:3655. https://doi.org/10.3390/ma15103655.

[60] Mondal MK, Mishra G, Kumar P. Adsorption of cadmium (II) and chromium (VI) from aqueous solution by waste marigold flowers. J Sustain Develop Energy Water Environ System. 2015; 3:405-415. https://doi.org/10.13044/j.sdewes.2015.03.0030.

[61] Upadhyay SK, Devi P, Kumar V, Pathak HK, Kumar P, Rajput VD, et al. Efficient removal of total arsenic (As3+/5+) from contaminated water by novel strategies mediated iron and plant extract activated waste flowers of marigold. Chemosphere. 2023; 313:137551. https://doi.org/10.1016/j.chemosphere.2022.137551.

[62] Prajapati AK, Mondal MK. Novel green strategy for CuO–ZnO–C nanocomposites fabrication using marigold (Tagetes spp.) flower petals extract with and without CTAB treatment for adsorption of Cr(VI) and Congo red dye. J Environ Manage. 2021; 290:112615. https://doi.org/10.1016/j.jenvman.2021.112615.

[63] Agarwal A, Kumar A, Gupta P, Tomar R, Singh NB. Cu (II) ions removal from water by charcoal obtained from marigold flower waste. Mater Today Proc. 2021;34:875-9. https://doi.org/10.1016/j.matpr.2020.11.046.

[64] Chang M. Research progress on calendula officinalis Pb/Cd compound pollution. J Phys Conf Ser. 2021; 1865:022023. https://doi.org/10.1088/1742-6596/1865/2/022023.

[65] Hasanin T, Ahmed S, Barakat T. Nano-chamomile waste as a low-cost biosorbent for rapid removal of heavy metal ions from natural water samples. Egypt J Chem. 2019;62(5): 937-953. https://doi.org/10.21608/ejchem.2019.5921.1504.

[66] Ahmed W, Mehmood S, Núñez-Delgado A, Ali S, Qaswar M, Shakoor A, et al. Adsorption of arsenic (III) from aqueous solution by a novel phosphorus-modified biochar obtained from Taraxacum mongolicum Hand-Mazz: Adsorption behavior and

mechanistic analysis. J Environ Manage. 2021; 292:112764. https://doi.org/10.1016/j.jenvman.2021.112764.

[67] Fuks L, Oszczak A, Dudek J, Majdan M, Trytek M. Removal of the radionuclides from aqueous solutions by biosorption on the roots of the dandelion (Taraxacum officinale). Inter J Environ Sci Technol. 2016; 13:2339-52. https://doi.org/10.1007/s13762-016-1067-3.

[68] Almasi A, Navazeshkha F, Mousavi SA. Biosorption of lead from aqueous solution onto Nasturtium officinale: performance and modelingBiosorption of lead from aqueous solution onto Nasturtium officinale: performance and modeling. Desalination Water Treat 2017; 65:443-50. https://doi.org/10.5004/dwt.2017.20308.

[69] Pourmanouchehri Z, Chahardoli A, Qalekhani F, Derakhshankhah H, Shokoohinia Y, Fattahi A, et al. Green modification of iron oxide nanoparticles with achillea wilhelmsii and investigation of their performance for methylene blue adsorption. J Nanostruct. 2022; 12:99-112. https://doi.org/10.22052/JNS.2022.01.010.